Title

Orbital Stability Analysis for Perturbed Nonlinear Systems and Natural Entrainment via Adaptive Andronov–Hopf Oscillator

Journal

IEEE Transactions on Automatic Control, 65(1)

ISSN

0018-9286

Authors

Zhao, Jinxin
Iwasaki, Tetsuya

Publication Date

2020

DOI

10.1109/tac.2019.2906429

Peer reviewed

Orbital Stability Analysis for Perturbed Nonlinear Systems and Natural Entrainment via Adaptive Andronov-Hopf Oscillator

Jinxin Zhao and Tetsuya Iwasaki

***Abstract*—Periodic orbits often describe desired state trajectories of dynamical systems in various engineering applications. Stability analysis of periodic solutions lays a foundation for control design to achieve convergence to a prescribed orbit. Here we consider a class of perturbed nonlinear systems with fast and slow dynamics and develop a novel averaging method for analyzing the local exponential orbital stability of a periodic solution. A framework is then proposed for feedback control design to stabilize a natural oscillation of an uncertain nonlinear system using a synchronous adaptive oscillator. The idea is applied to linear mechanical systems and a design theory is established. In particular, we propose a controller based on the Andronov-Hopf oscillator with additional adaptation mechanisms for estimating the unknown natural frequency and damping parameters. We prove that, with sufficiently slow adaptation, the estimated parameters locally converge to their true values and entrainment to the natural oscillation is achieved as part of an orbitally stable limit cycle. Numerical examples demonstrate that adaptation and convergence can in fact be fast.**

I. Introduction

Feedback control design to achieve oscillations is important in many engineering applications. Such designs are useful for repetitive motion control for industrial manipulators, and have also been implemented in other tasks such as legged locomotion [1], [2] and human assistive exoskeleton [3], [4]. In these applications, dedicated trajectory planning and high gain servo tracking have been extensively used, as exemplified by the output regulation theory [5]. The traditional method allows for fast and precise motion, but the target trajectory is fixed *a priori*. As a result, robotic devices driven by such control algorithms are not adaptive nor compliant to varying environment and may have high energy consumption [6]. Approaches based on shaping the zero dynamics [7], [8] allow for adjustment of phase timing in response to disturbances, but the target motion is still fixed as a manifold in the state space specified by holonomic constraints.

During the past decades, compliant actuators have drawn increasing attention of engineers in robotic fields since the seminal work on series elastic actuators [9], which have dynamics analogous to muscles. This kind of robotic mechanism is able to increase the efficiency by storing kinetic energy as potential energy to be used for the next cycle, like their counterpart, muscle, does in animal movements. Numerous robots with compliant actuators have been developed. For example, bipedal and quadrupedal robots driven by compliant actuators achieve natural and energy-efficient walking motion [10]–[13]. Similarly, a tensegrity structure [14] has been used [15], [16] for compliant actuation of a robotic fish to exploit resonance for efficient swimming. Other applications include lower-limb exoskeletons with built-in compliance [17], [18] to perform safe and smooth movements. Thus, there is a trend in the control of robots from highly stiff and precise trajectory tracking towards soft and compliant motion exploiting the intrinsic dynamics of the system to achieve high energy-efficiency and natural movements.

Exploitation of natural dynamics is common in biological control systems for rhythmic body movements. Resonance is exploited to achieve high efficiency for instance in fish swimming [19], walking and running [20], [21], and periodic forearm motion [22]. Such movements are controlled by the central pattern generator (CPG), which is a nonlinear oscillator formed by neuronal circuits. CPGs have been shown to have the ability to detect and tune into the mechanical resonance [23]–[27]. The CPG mechanisms have been used for designing bio-inspired controllers to achieve adaptive entrainment to a natural mode of oscillations for mechanical systems [28], [29] or provide assistive force to help human make oscillatory movement [30]. Furthermore, learning methods have been combined with the CPG to include explicit mechanisms for frequency adaptation [31], [32], one of which is implemented in a quadruped robot to exploit a resonance [33]. While the CPG-based methods were found effective for certain cases, no theoretical guarantee for convergence was provided. The method of feedback resonance [34], [35] has convergence proofs, but the control law is discontinuous and the system is restricted to those with Rayleigh damping. Despite these numerous attempts, it remains open to establish systematic and effective control design methods for exploiting unknown natural dynamics of general mechanical systems.

In this paper, we will first develop a general framework for stability analysis and control synthesis for periodic orbits of a class of perturbed nonlinear systems. Our approach is based on linearization of the system around a periodic orbit and Floquet analysis of the resulting linear periodic system. A simple condition for orbital stability is developed, using an averaging technique and perturbation analysis. A feedback control architecture is then proposed to achieve a natural oscillation for uncertain nonlinear systems. The controller is based on a nonlinear oscillator that synchronizes with the plant through weak coupling and slow adaptation mechanisms. The control architecture yields the closed-loop system that fits the analysis framework of perturbed nonlinear systems.

The framework is applied to a general class of uncertain linear mechanical systems with multiple degrees of freedom

This work is supported by NSF grant No.1427313.

Jinxin Zhao and Tetsuya Iwasaki are with the Department of Mechanical and Aerospace Engineering, University of California, Los Angeles, California. Email: {jinxinzh,tiwasaki}@ucla.edu.

(DOF), and a method is proposed for designing a controller to achieve exact entrainment to a selected mode of natural oscillations with a theoretical guarantee for convergence. To this end, we first develop an oscillator that synchronizes with the external sinusoidal input, using the Andronov-Hopf oscillator (AHO) as the basic structure with additional adaptation mechanisms to tune the frequency parameter. We then modify the adaptive AHO to include a damping estimation mechanism, place it in the feedback loop with a single-DOF mechanical system, and show that the closed-loop system has an exponentially stable limit cycle on which the natural oscillation is achieved. Finally, we will extend the result for multi-DOF mechanical systems. Although convergence is guaranteed only when adaptation is sufficiently slow, numerical examples demonstrate that the target orbit remains stable when the perturbation parameters are large, and thus fast convergence can be achieved.

Preliminary results of this article were presented at a conference [36] without proofs. Here, the adaptation mechanisms and stability conditions are much simplified and improved for faster convergence. All the results are rigorously proven and numerical examples are fully renewed for better illustration.

II. General Framework

In this section, we consider a class of perturbed nonlinear systems and develop a general framework for stability analysis of periodic solutions as well as for their synthesis by feedback control. We employ a classical approach (e.g. [37]) to separate and average the slow dynamics in the neighborhood of the periodic orbit, and provide a new condition for exponential stability of the orbit in the limiting case. The technical tool developed here will be used in later analyses.

A. Preliminaries

Let us first introduce two notions of stability.

Definition 1: Consider a dynamical system $\dot{\mathrm{x}} = \mathfrak{f}(t, \mathrm{x})$ and a solution $\mathrm{x} = \xi$, where both $\mathfrak{f}(\cdot, \mathrm{x})$ and $\xi(\cdot)$ are T-periodic. The solution ξ is said to be exponentially stable if there exist positive constants c_1, c_2, and c_3, independent of t_o, such that

$$\|\mathrm{x}(t) - \xi(t)\| \le c_1 \|\mathrm{x}(t_o) - \xi(t_o)\| e^{-c_2(t-t_o)}$$

holds for all $t \ge t_o \ge 0$, whenever $\|\mathrm{x}(t_o) - \xi(t_o)\| < c_3$. Suppose the system is autonomous, and define the orbit $\mathbb{O}$ and the distance to $\mathbb{O}$ by

$$\mathbb{O} := \{\ \xi(t) \in \mathbb{R}^n :\ t \in \mathbb{R}\ \}, \quad d(\mathrm{x}, \mathbb{O}) := \min_{\mathrm{y} \in \mathbb{O}} \|\mathrm{x} - \mathrm{y}\|.$$

The solution ξ is said to be orbitally exponentially stable if there exist positive constants c_1, c_2, and c_3 such that

$$d(x(t), \mathbb{O}) \le d(x(0), \mathbb{O}) c_1 e^{-c_2 t}$$

holds for all $t \ge 0$, whenever $d(x(0), \mathbb{O}) < c_3$.

Here, the stability of a solution $\mathrm{x} = \xi$ is defined in accordance with the stability of an equilibrium $\nu = 0$ of the new system obtained by coordinate transformation $\nu := \mathrm{x} - \xi$. This type of definition has been used for example in [38], p.314, and [39], p.133. The above definition of orbital stability is standard [39], [40]. The orbital exponential stability actually implies existence of an asymptotic phase c such that $\|\mathrm{x}(t) - \xi(t + c)\|$ converges exponentially to zero ([41], p.254, Theorem 11.1).

It is well known that the origin is an exponentially stable equilibrium point of $\dot{\mathrm{x}} = \mathfrak{f}(t, \mathrm{x})$ (where $\mathfrak{f}$ is not necessarily periodic, but continuously differentiable and Lipschitz) if and only if the origin is an exponentially stable equilibrium point of the linearization around the origin ([39], p.152, Theorem 3.13). As a corollary, a solution ξ is exponentially stable if and only if $\dot{\nu} = \frac{\partial \mathfrak{f}}{\partial \mathrm{x}}(t, \xi)\nu$ is exponentially stable. When $\mathfrak{f}$ and ξ are T-periodic, the solution ξ is exponentially stable if and only if all the Floquet multipliers of $A(t) := \frac{\partial \mathfrak{f}}{\partial \mathrm{x}}(t, \xi)$ are strictly inside the unit circle [42]. The orbital stability of ξ can be examined similarly. The periodic solution ξ of $\dot{\mathrm{x}} = \mathfrak{f}(\mathrm{x})$ is orbitally exponentially stable if and only if all but one of the Floquet multipliers of the linearized system $\dot{\nu} = \frac{\partial \mathfrak{f}}{\partial \mathrm{x}}(\xi)\nu$ have magnitudes strictly less than one ([40], Theorem 1.1).

B. Stability Analysis of Perturbed Nonlinear Oscillator

Consider a nonlinear system

$$\begin{aligned} \dot{\chi} &= \mathsf{f}(\chi, y, t) + \varepsilon \mathsf{h}(\chi, y, t) \\ \dot{y} &= \varepsilon \mathsf{g}(\chi, y, t) \end{aligned} \tag{1}$$

where (χ, y) are the states, $\varepsilon \in \mathbb{R}$ is a perturbation parameter, and functions $\mathsf{f}, \mathsf{g}, \mathsf{h}$ are periodic in t with period $T > 0$ (or the system may be time invariant). We consider the case where $\varepsilon > 0$ is small, and y slowly changes its value over time. The variable χ with fast dynamics and y with slow dynamics are mutually coupled. Suppose the system has a T-periodic (or constant) solution (χ_o, y_o). The linearization of the system (1) around the solution yields a linear periodic system

$$\begin{bmatrix} \dot{\tilde{\chi}} \\ \dot{\tilde{y}} \end{bmatrix} = \begin{bmatrix} A_1(t) + \varepsilon B_1(t) & A_2(t) + \varepsilon B_2(t) \\ \varepsilon C_1(t) & \varepsilon C_2(t) \end{bmatrix} \begin{bmatrix} \tilde{\chi} \\ \tilde{y} \end{bmatrix}, \tag{2}$$

where

$$\begin{aligned} &\tilde{\chi} := \chi - \chi_o, \quad \tilde{y} := y - y_o, \\ &A_1(t) = \frac{\partial \mathsf{f}}{\partial \chi}, \quad B_1(t) = \frac{\partial \mathsf{h}}{\partial \chi}, \quad C_1(t) = \frac{\partial \mathsf{g}}{\partial \chi}, \\ &A_2(t) = \frac{\partial \mathsf{f}}{\partial y}, \quad B_2(t) = \frac{\partial \mathsf{h}}{\partial y}, \quad C_2(t) = \frac{\partial \mathsf{g}}{\partial y}, \end{aligned}$$

with the partial derivatives evaluated at (χ_o, y_o, t). Note that all the coefficient matrices are T-periodic.

The solution (χ_o, y_o) is exponentially stable if and only if the linear periodic system (2) is exponentially stable . However, exponential stability of the linear system is not required for orbital exponential stability of (χ_o, y_o). In fact, (2) can never be exponentially stable if the original nonlinear system (1) is time-invariant and the solution is not constant since $(\tilde{\chi}, \tilde{y}) = (\dot{\chi}_o, \dot{y}_o)$ is a solution of the linear system not converging to the origin. In this case, the non-convergent mode can be isolated by a coordinate transformation and then orbital exponential stability of (χ_o, y_o) is implied by exponential stability of the remaining part of the system. This idea was used in [43] for a coupled oscillator problem, and will also be used later in this paper for the natural entrainment problem. The reduced system turns out to have the same form as (2). Thus, for both stability and orbital stability of periodic

solutions (or equilibria), a fundamental problem is the stability analysis of the linear periodic (or time-invariant) system of the form (2).

A general method for analyzing stability of linear periodic systems is to use the Floquet multiplier. While computing the Floquet multipliers is straightforward, the analysis is numerical and the method is not suitable for analytical development of design conditions for guaranteed stability. Here we propose an alternative method for stability analysis exploiting the structure of the linear periodic system.

A simple stability condition is obtained if the two variables $(\tilde{\chi}, \tilde{y})$ in (2) are decoupled. Consider a linear transformation

$$\begin{bmatrix} w \\ \tilde{y} \end{bmatrix} = \begin{bmatrix} I & -\mathcal{L}_\varepsilon(t) \\ 0 & I \end{bmatrix} \begin{bmatrix} \tilde{\chi} \\ \tilde{y} \end{bmatrix} \tag{3}$$

where $\mathcal{L}_\varepsilon(t)$ is a matrix-valued differentiable function of time, depending on the perturbation parameter ε. Let us choose $\mathcal{L}_\varepsilon(t)$ such that

$$\dot{\mathcal{L}}_\varepsilon(t) = A_1(t)\mathcal{L}_\varepsilon(t) + A_2(t) + \varepsilon G(t, \mathcal{L}_\varepsilon(t)), \tag{4}$$

where

$$G(t, X) := B_2(t) + B_1(t)X - XC_2(t) - XC_1(t)X. \tag{5}$$

Then the system can be described as

$$\begin{bmatrix} \dot{w} \\ \dot{\tilde{y}} \end{bmatrix} = \begin{bmatrix} \mathcal{A}_1(t) & 0 \\ \varepsilon C_1(t) & \varepsilon(C_2(t) + C_1(t)\mathcal{L}_\varepsilon(t)) \end{bmatrix} \begin{bmatrix} w \\ \tilde{y} \end{bmatrix} \tag{6}$$

where the (1,2) block of the coefficient matrix is made equal to zero by the choice of $\mathcal{L}_\varepsilon(t)$, and

$$\mathcal{A}_1(t) := A_1(t) + \varepsilon(B_1(t) - \mathcal{L}_\varepsilon(t)C_1(t)).$$

Now the original linear periodic system (2) is transformed into system (6), where the fast dynamics w is decoupled from the slow dynamics $\tilde{y}$. With the help of the separation, we can examine stability of the original system (2) by analyzing the two subsystems associated with w and $\tilde{y}$. Furthermore, when $|\varepsilon|$ is sufficiently small, we may approximate $\mathcal{A}_1$ by A_1, and $\mathcal{L}_\varepsilon$ by $\mathcal{L}_o$ satisfying

$$\dot{\mathcal{L}}_o(t) = A_1(t)\mathcal{L}_o(t) + A_2(t). \tag{7}$$

This idea leads to the following result.

Lemma 1: Consider the linear T-periodic (or time-invariant) system (2), where all the coefficient matrices are continuous and bounded functions of time. Suppose there exists a solution $\mathcal{L}_o(t)$ to (7) that is T-periodic or constant, and define

$$\mathcal{B} := \int_0^T \big(C_2(t) + C_1(t)\mathcal{L}_o(t)\big)dt. \tag{8}$$

If the system $\dot{x} = A_1(t)x$ is exponentially stable and $\mathcal{B}$ is Hurwitz, then there exists $\bar{\varepsilon}$ such that system (2) is exponentially stable for all $\varepsilon \in (0, \bar{\varepsilon})$.

Proof: For each $\varepsilon > 0$, let $\mathcal{L}_\varepsilon(t)$ be the solution to (4) with initial condition $\mathcal{L}_\varepsilon(0) = \mathcal{L}_o(0)$, and define $\Delta_\varepsilon(t)$ by

$$\mathcal{L}_\varepsilon(t) = \mathcal{L}_o(t) + \varepsilon\Delta_\varepsilon(t). \tag{9}$$

By Lemma 3 in the appendix, there exists $\bar{\varepsilon}_1 > 0$ such that $\mathcal{L}_\varepsilon$ and Δ_ε with $\varepsilon \in (0, \bar{\varepsilon}_1)$ are bounded and continuously differentiable when $\dot{x} = A_1(t)x$ is exponentially stable. Then, through the Lyapunov transformation introduced in (3), two systems (2) and (6) are equivalent when $\varepsilon \in (0, \bar{\varepsilon}_1)$. The stability of system (6) depends on two separate systems

$$\dot{w} = \Big(A_1(t) + \varepsilon(B_1(t) - \mathcal{L}_\varepsilon(t)C_1(t))\Big)w, \tag{10}$$

$$\dot{\tilde{y}} = \varepsilon\Big(C_2(t) + C_1(t)\mathcal{L}_\varepsilon(t)\Big)\tilde{y}. \tag{11}$$

Based on Lemma 4 in the appendix, there exists $\bar{\varepsilon}_2$ such that system (10) is exponentially stable for all $\varepsilon \in (0, \bar{\varepsilon}_2)$ due to exponential stability of $A_1(t)$ and boundedness of the perturbation term multiplied by ε. The system (11) can be rewritten as

$$\dot{\tilde{y}} = \varepsilon\Big(C_2(t) + C_1(t)\mathcal{L}_o(t) + \varepsilon C_1(t)\Delta_\varepsilon(t)\Big)\tilde{y}. \tag{12}$$

By Lemma 5, there exists $\bar{\varepsilon}_3 > 0$ such that system (12) is exponentially stable for all $\varepsilon \in (0, \bar{\varepsilon}_3)$ since $\mathcal{B}$ in (8) is Hurwitz and C_1 and Δ_ε are bounded. ■

C. Control Design for Stable Oscillation

We propose a feedback control design framework based on the above analysis to achieve a desired oscillation as an orbitally stable limit cycle of the closed-loop system. Consider the nonlinear plant described by

$$\dot{\zeta} = p(\zeta, u), \quad z = q(\zeta),$$

where ζ is the state, u is the control input, and z is the output. Suppose a state feedback control $u = r(\zeta, \theta)$ makes a given periodic trajectory $\zeta = \zeta_o$ a (not necessarily stable) solution of the closed-loop system, where θ is a vector of the plant parameters on which the control law depends. The objective is to design an output feedback controller so that the closed-loop system has a stable limit cycle on which $\zeta = \zeta_o$ is achieved. A complication is that the value of θ is unknown.

An approach is to use the control architecture based on a synchronous adaptive oscillator:

$$\dot{x} = o(x, y) + \varepsilon c(x, z), \quad \dot{y} = \varepsilon g(x, z), \quad u = r(s(x), y).$$

The function o is chosen so that $\dot{x} = o(x, \theta)$ is a nonlinear oscillator with an orbitally stable limit cycle $x = x_o$ to generate the target oscillation by $\zeta_o = s(x_o)$. The function c couples the plant and the oscillator to achieve synchronization, $x(t) \to x_o(t + a)$ with $a = 0$, when $z = q(\zeta_o)$ and $y = \theta$. The function g vanishes on the target orbit $g(x_o, q(\zeta_o)) = 0$ and defines an adaptation mechanism that makes y converge to θ by detecting the error $y \neq \theta$ through $(x, z) \neq (x_o, q(\zeta_o))$.

The closed-loop system takes the form (1) with $\chi := \mathrm{col}(\zeta, x)$ and orbital stability of the target limit cycle $(\zeta, x, y) = (\zeta_o, x_o, \theta)$ can be analyzed using Lemma 1, where the small parameter ε yields slow adaptation and facilitates the convergence analysis. In the following sections, the general framework for orbital stability analysis and synthesis described here will provide a helpful guidance for designing an adaptive oscillator and natural entrainment controller for linear mechanical systems.

III. Adaptive Oscillator

A. Problem Formulation

We first consider, as a basis for later developments, the problem of designing an oscillator that synchronizes to an external periodic signal in an adaptive manner. In particular, the system to be designed comprises a nonlinear oscillator and an adaptation mechanism that dynamically modifies oscillator parameters based on the periodic input. The trajectory of the adaptive oscillator will converge locally to a periodic orbit on which one of the oscillator variables is synchronized with the periodic input, and the adaptation variables are constant with values at the frequency and amplitude of the input. A formal statement of the problem is the following.

Problem 1: Let $z(t)$ be a T-periodic sinusoidal signal

$$z(t) = \alpha \sin(\omega t) \tag{13}$$

where $\alpha, \omega \in \mathbb{R}$ are unknown amplitude and frequency, and $T := 2\pi/\omega$. Design an adaptive nonlinear oscillator

$$\dot{x} = f(x, y, z), \quad \dot{y} = g(x, y, z), \quad v = h(x), \tag{14}$$

where $(x, y) \in \mathbb{R}^n \times \mathbb{R}^m$ is the state vector, and $v \in \mathbb{R}$ is the output signal, to satisfy the following specifications:

(i) There exists an exponentially stable solution (x, y) to (14) such that

$$x(t) = x(t + T), \quad y(t) \equiv \mathrm{col}(\omega, \alpha), \quad v(t) = z(t).$$

(ii) The oscillator dynamics f, g, and h are independent of the signal parameters (ω, α).

B. Approach

Our approach to solve Problem 1 is to exploit the structure of the Andronov-Hopf oscillator with additional adaptation mechanisms. The AHO is a simple planar nonlinear oscillator, in which every nontrivial trajectory converges to a single limit cycle. The orbit in the state space is circular, and the time courses of the state variables are sinusoidal. The amplitude and frequency of the oscillation are directly specified by certain model parameters. More specifically, AHO is described as

$$\begin{bmatrix} \dot{x}_1 \\ \dot{x}_2 \end{bmatrix} = \begin{bmatrix} \sigma(x_1, x_2) & \omega \\ -\omega & \sigma(x_1, x_2) \end{bmatrix} \begin{bmatrix} x_1 \\ x_2 \end{bmatrix}, \tag{15}$$
$$\sigma(x_1, x_2) := \mu(\varrho - x_1^2 - x_2^2)$$

where $x_i(t) \in \mathbb{R}$ for $i = 1, 2$ are the states, ϱ and ω are the amplitude and frequency parameters, respectively, and $\mu > 0$ specifies the convergence rate. When σ is zero, the AHO is a linear (undamped) oscillator. The nonlinear function σ provides positive/negative damping when the oscillation amplitude $x_1^2 + x_2^2$ is larger/smaller than ϱ. In particular, the origin is globally exponentially stable when $\varrho < 0$, and as ϱ transitions to a positive value, a Hopf bifurcation occurs at $\varrho = 0$ and a stable limit cycle of amplitude $\|x\| = \sqrt{\varrho}$ emerges. Precise analysis is rather simple. Introducing the polar coordinates

$$\begin{bmatrix} x_1 \\ x_2 \end{bmatrix} = \begin{bmatrix} r \sin\theta \\ r \cos\theta \end{bmatrix}, \tag{16}$$

system (15) is expressed as

$$\dot{r} = \mu(\varrho - r^2)r, \quad \dot{\theta} = \omega.$$

It is then easy to see that the amplitude $r(t)$ will converge to zero if $\varrho \leq 0$, or otherwise to $\pm\alpha$ unless $r(0) = 0$ where $\alpha := \sqrt{\varrho}$, and the phase $\theta(t)$ is given by $\theta(t) = \omega t + \theta(0)$. Thus, when $\varrho > 0$, the sinusoidal trajectory

$$\begin{bmatrix} x_1 \\ x_2 \end{bmatrix} = \begin{bmatrix} \alpha \sin\omega t \\ \alpha \cos\omega t \end{bmatrix}$$

is an orbitally exponentially stable solution of the system (15).

We design an adaptive oscillator using the AHO as the starting point. Since ω and α are unknown in Problem 1, we replace (ω, α) in (15) with (y_1, y_2) as the variables to be adjusted so that they converge to the frequency and amplitude of z. A natural choice for the output is $q := x_1$, and we drive the AHO by the error $z - x_1$ to achieve synchronization $q = z$. Overall, we add the following adaptation mechanism to the dynamics of Andronov-Hopf oscillator:

$$\begin{bmatrix} \dot{x}_1 \\ \dot{x}_2 \end{bmatrix} = \begin{bmatrix} \sigma & y_1 \\ -y_1 & \sigma \end{bmatrix} \begin{bmatrix} x_1 \\ x_2 \end{bmatrix} + \gamma \begin{bmatrix} z - x_1 \\ 0 \end{bmatrix} \tag{17a}$$

$$\dot{y}_1 = \eta x_2 (z - x_1), \tag{17b}$$

$$\dot{y}_2 = \kappa(z^2 + x_2^2 - y_2^2) \tag{17c}$$

$$\sigma := \mu(y_2^2 - x_1^2 - x_2^2), \tag{17d}$$

where $\gamma, \eta, \kappa, \mu \in \mathbb{R}$ are positive constants, and (x_1, x_2, y_1, y_2) are the states of the oscillator. It is designed such that $x_1(t)$ synchronizes with the signal $z(t)$, while (y_1, y_2) converges to (ω, α). The parameters μ and γ specify the convergence rates of the oscillation amplitude and synchronization, and η and κ specify the rates of adaptation of frequency and amplitude.

The idea behind the adaptation mechanism is as follows. It is easy to verify that, if $y_1(t) \equiv \omega$ and $\mu = 0$ in (17a), then the linear system driven by the error signal converges to a sinusoidal trajectory on which $x_1 = z$. It turns out that the convergence property is maintained when the nonlinearity in the AHO becomes active (i.e., $\mu > 0$), provided $y_2(t) \equiv \alpha$. The mechanism in (17c) increases/decreases the estimated amplitude y_2 when the actual amplitude $\sqrt{z^2 + x_2^2}$ is larger/smaller than the current estimate y_2. Finally, the mechanism in (17b) increases/decreases the estimated frequency y_1 when the phase of x_1 is behind/advance with respect to z. In particular, with x in (16), we have

$$x_2(z - x_1) \cong -(\alpha \cos\omega t)^2 \varphi + O(\varphi^2), \quad \varphi := \theta - \omega t,$$

provided the amplitude is correct; $r = \alpha$. Thus, assuming the phase difference $|\varphi|$ is small, $\dot{y}_1$ is positive/negative when z is ahead/behind of x_1, which causes an increase/decrease of y_1 and acceleration/deceleration of x_1. Eventually, z and x_1 will have no phase difference and synchronize. These intuitive ideas are rigorously verified to work in the next subsection.

C. Result

The following theorem provides a formal statement of a sufficient condition for synchronization of the adaptive oscillator.

Theorem 1: Consider the adaptive oscillator (17) is connected with a sinusoidal signal (13). Suppose $\gamma, \eta, \kappa \in \mathbb{R}$ are positive and $\mu \in \mathbb{R}$ is nonnegative. Then there exists $\bar{\varepsilon}$ such that the state trajectory

$$(x_1, x_2, y_1, y_2) = (\alpha \sin(\omega t), \alpha \cos(\omega t), \omega, \alpha) \tag{18}$$

is exponentially stable whenever η, κ, μ are smaller than $\bar{\varepsilon}$.

Proof: It is straightforward to verify that the signal in (18) is a solution of the system. Let the small parameters be expressed as

$$\begin{bmatrix} \eta & \kappa & \mu \end{bmatrix} = \varepsilon \begin{bmatrix} \tilde{\eta} & \tilde{\kappa}/4 & \tilde{\mu}/4 \end{bmatrix}$$

with small $\varepsilon > 0$. Introducing the perturbation variables

$$\begin{aligned} \tilde{x}_1 &:= x_1 - \alpha s, \quad \tilde{y}_1 := y_1 - \omega, \quad s := \sin(\omega t), \\ \tilde{x}_2 &:= x_2 - \alpha c, \quad \tilde{y}_2 := y_2 - \alpha, \quad c := \cos(\omega t), \end{aligned}$$

the linearized system is given by

$$\dot{\tilde{x}} = \begin{bmatrix} A_1 + \varepsilon B_1 & A_2 + \varepsilon B_2 \\ \varepsilon C_1 & \varepsilon C_2 \end{bmatrix} \tilde{x},$$

where

$$\begin{bmatrix} A_1 & A_2 \\ C_1 & C_2 \end{bmatrix} := \left[\begin{array}{cc|cc} -\gamma & \omega & \alpha c & 0 \\ -\omega & 0 & -\alpha s & 0 \\ \hline -\tilde{\eta}\alpha c & 0 & 0 & 0 \\ 0 & \tilde{\kappa}\alpha c & 0 & -\tilde{\kappa}\alpha \end{array}\right],$$

$$\begin{bmatrix} B_1 & B_2 \end{bmatrix} := -\tilde{\mu}\alpha^2 \left[\begin{array}{cc|cc} s^2 & sc & 0 & -s \\ sc & c^2 & 0 & -c \end{array}\right].$$

It is easy to verify that A_1 is Hurwitz, and the periodic solution $\mathcal{L}_o$ to

$$\dot{\mathcal{L}}_o = A_1 \mathcal{L}_o + A_2$$

exists and is given by

$$\begin{aligned} \mathcal{L}_o &= \Re[\hat{\mathcal{L}}_o e^{j\omega t}], \quad \hat{A}_2 := \begin{bmatrix} \alpha & 0 \\ \alpha j & 0 \end{bmatrix}, \\ \hat{\mathcal{L}}_o &:= (j\omega I - A_1)^{-1} \hat{A}_2 = \frac{\alpha}{\omega\gamma} \begin{bmatrix} 2\omega & 0 \\ \gamma + 2j\omega & 0 \end{bmatrix} \end{aligned}$$

Noting that

$$\begin{aligned} \mathcal{B} &= \frac{1}{T}\int_0^T \Big(C_1 \mathcal{L}_o + C_2\Big) dt = \frac{1}{2}\Re\Big(\hat{C}_1 \hat{\mathcal{L}}_o\Big) + C_2 \\ &= \begin{bmatrix} -\alpha^2\tilde{\eta}/\gamma & 0 \\ \alpha^2\tilde{\kappa}/(2\omega) & -\alpha\tilde{\kappa} \end{bmatrix}, \quad \hat{C}_1 := \alpha \begin{bmatrix} -\tilde{\eta} & 0 \\ 0 & \tilde{\kappa} \end{bmatrix}, \end{aligned}$$

and $\mathcal{B}$ is Hurwitz, we conclude the result. ∎

Theorem 1 provides an approach to design the oscillator dynamics to adaptively synchronize with an external sinusoidal signal. Synchronization is asymptotically achieved as long as the adaptation of the frequency and amplitude variables is sufficiently slow. Moreover, the system is designed to sustain, after the convergence, the oscillation in a stable and autonomous manner without the input (i.e., $\gamma = 0$), and therefore the process can be seen as learning of a training periodic signal by a nonlinear oscillator. For practical purposes, the convergence rate can be made fast by adjusting the adaptation parameters η, κ and μ. A numerical example in Section VI illustrates this point in comparison with an existing method. Noting that $\mu = 0$ is a valid choice for the design, the nonlinearity σ is not essential for the convergence property of the adaptive oscillator. However, it will play a crucial role when we extend the result to consider a feedback control problem in the next section.

IV. Adaptive Natural Entrainment

A. Problem Formulation

We consider a single degree-of-freedom mechanical system with unknown parameters and develop a method for designing a feedback controller to achieve the natural oscillation of the system. The control architecture is based on the adaptive oscillator described in the previous section. The single-DOF result provides a comprehensive explanation of the idea for closing the loop and embedding an exponentially stable limit cycle in the state space, and sets a stage for multi-DOF extension in the next section.

Let a mechanical system be given by

$$m\ddot{z} + d\dot{z} + kz = u, \tag{19}$$

where $m, d, k \in \mathbb{R}$ are positive parameters representing the mass, damping and stiffness, $u(t) \in \mathbb{R}$ is the force input from an actuator, and $z(t) \in \mathbb{R}$ is the resulting displacement. The natural oscillation of the system is defined as

$$z_n(t) = \alpha \sin(\varpi t), \quad \varpi := \sqrt{k/m}, \tag{20}$$

where ϖ is the undamped natural frequency of the system, and $\alpha \in \mathbb{R}$ is the amplitude of z_n. Let $T := 2\pi/\varpi$ be the natural period.

We aim to design a feedback controller that achieves local convergence of $z(t)$ to $z_n(t + c)$ in the steady state, where the oscillation amplitude α is assigned by the controller while the constant c depends on the initial state of the closed-loop system. In addition, we would like the controller to be adaptive in the sense that the controller meets the objective with no information of the system parameters m, d and k. A formal statement of the design problem is as follows.

Problem 2: Let a mechanical system in (19) and a positive scalar $\alpha \in \mathbb{R}$ be given, and consider the natural oscillation z_n defined in (20). Design a feedback controller of the form

$$\dot{x} = f(x, y, z), \quad \dot{y} = g(x, z), \quad u = h(x, y),$$

where $(x, y) \in \mathbb{R}^n \times \mathbb{R}^m$ is the state vector, to achieve the natural oscillation with amplitude α in the steady state. In particular, the design specifications are the following:

(i) There exists an orbitally exponentially stable solution $(x, y, z, \dot{z})$ of the closed-loop system such that

$$x(t) = x(t + T), \quad y(t) \equiv \mathrm{col}(\varpi, d), \quad z = z_n.$$

(ii) Functions f, g and h specifying the controller are independent of the system parameters m, d, and k.

This is an adaptive natural entrainment problem where a controller is sought to adaptively achieve entrainment to the natural oscillation. The adaptation variable y should estimate

all the unknown system parameters necessary for the natural entrainment, and it turns out that estimation of the natural frequency ϖ and the damping coefficient d is sufficient for the purpose as explained in the next section.

B. Approach

The basic idea for solving Problem 2 is the following. When the control objective is met, the natural oscillation $z = z_n$ is achieved for (19). This necessitates $u = d\dot{z}_n$ in the steady state. To make this happen, the first step is to drive the AHO by mechanical variable z and add an adaptation mechanism so that the parameter ω is adjusted in real time and converge to the natural frequency ϖ of the mechanical system when $z = z_n$. The second step is to add another mechanism to estimate the mechanical damping d, and close the loop by setting the control input u to compensate for the damping.

These two steps are accomplished by placing the adaptive oscillator (17) in the feedback loop, with modifications to estimate d and generate u. In particular, we consider the following AHO based feedback controller

$$\begin{bmatrix}\dot{x}_1\\ \dot{x}_2\end{bmatrix} = \begin{bmatrix}\sigma & y_1\\ -y_1 & \sigma\end{bmatrix}\begin{bmatrix}x_1\\ x_2\end{bmatrix} + \gamma\begin{bmatrix}z - x_1\\ 0\end{bmatrix} \tag{21a}$$

$$\dot{y}_1 = \eta x_2(z - x_1), \tag{21b}$$

$$\dot{y}_2 = \kappa(\alpha^2 - z^2 - x_2^2) \tag{21c}$$

$$u = x_2 y_1 y_2, \quad \sigma := \mu(\alpha^2 - x_1^2 - x_2^2), \tag{21d}$$

where $\gamma, \eta, \kappa, \mu \in \mathbb{R}$ are positive constants, and $x_1(t)$ through $y_2(t)$ are the states of the controller. The controller (21) turns out to solve Problem 2, achieving entrainment to the natural oscillation of (19). The controller is designed so that x_1 and x_2 synchronize with the plant states z and $\dot{z}/\varpi$, respectively, while y_1 and y_2 estimate the natural frequency ϖ and damping coefficient d, respectively. The parameters γ and μ specify the rates of convergence for the amplitude and synchronization, and η and κ specify the rates of adaptation for frequency and damping, respectively. The underlying mechanism can be roughly explained as follows.

First, (21a) and (21b) form an adaptive oscillator with a frequency estimator similarly to the previous development. If $z(t)$ oscillates sinusoidally with frequency ϖ and amplitude α, (21a) stably generates sinusoidal signals $(x_1, x_2) = (\alpha\sin(\varpi t), \alpha\cos(\varpi t))$ so that $x_1 = z$, while (21b) makes y_1 converge to the natural frequency ϖ. In this case, the control input in (21d) is $u = y_2\dot{z}$. Based on (21c), the variable y_2 estimates the damping coefficient and converges to d by the following mechanism. If y_2 is larger/smaller than d, then system (19) under the control input has negative/positive damping, leading to larger/smaller amplitude of oscillation. If the amplitude becomes larger/smaller than α, the dynamics of (21c) decrease/increase the estimated damping y_2. Hence y_2 is regulated around the value d. In this case, the control input is $u = d\dot{z}$. From (19), we see that z satisfies $m\ddot{z} + kz = 0$ and therefore oscillates with natural frequency ϖ.

C. Result

The following theorem presents a formal statement of the result and gives a sufficient condition for entrainment to the natural oscillation.

Theorem 2: Consider mechanical system (19) and the feedback controller given by (21). Suppose the plant parameters m, d, k and controller parameters $\alpha, \mu, \gamma, \eta, \kappa \in \mathbb{R}$ are positive constants. Then

$$\begin{aligned}&\mathrm{col}(z, \dot{z}, x_1, x_2, y_1, y_2)\\ &= \mathrm{col}(z_n, \dot{z}_n, \alpha\sin\varpi t, \alpha\cos\varpi t, \varpi, d)\end{aligned} \tag{22}$$

is a solution of the closed-loop system. Moreover, there exists $\bar{\varepsilon} > 0$ such that the solution is orbitally exponentially stable whenever γ, η, and κ are smaller than $\bar{\varepsilon}$.

Proof: It is easily verified that (22) is a solution of the closed-loop system. Let normalized controller parameters be defined by

$$\varepsilon\begin{bmatrix}\tilde{\gamma} & \tilde{\eta} & \tilde{\kappa}\end{bmatrix} := \begin{bmatrix}\gamma & \eta\alpha^2 & 2\kappa\alpha^2\varpi\end{bmatrix}, \quad \tilde{\mu} := 2\mu\alpha^2.$$

Orbital exponential stability will be proven for the case where $\tilde{\gamma}$, $\tilde{\eta}$, $\tilde{\kappa}$, and $\tilde{\mu}$ are arbitrary positive constants and $\varepsilon > 0$ is sufficiently small. Using the polar coordinates and error variables

$$\begin{aligned}x_1 &= r\sin\theta, \quad e_1 = z_n - x_1,\\ x_2 &= r\cos\theta, \quad e_2 = \dot{z}_n - \varpi x_2,\end{aligned}$$

define a new state vector (θ, ξ) with

$$\xi := \mathrm{col}(r, e_1, e_2, \alpha y_1, \alpha\varpi y_2).$$

The trajectory (22) can then be given by

$$\theta = \varpi t, \quad \xi = \mathrm{col}(\alpha, 0, 0, \alpha\varpi, \alpha\varpi d). \tag{23}$$

Linearizing the closed-loop system around the solution (23), the resulting system is

$$\begin{bmatrix}\dot{\tilde{\theta}}\\ \dot{\tilde{\xi}}\end{bmatrix} = \begin{bmatrix}0 & b\\ 0 & \Sigma\end{bmatrix}\begin{bmatrix}\tilde{\theta}\\ \tilde{\xi}\end{bmatrix}, \quad \tilde{\xi} = \mathrm{col}(\tilde{r}, e_1, e_2, \alpha\tilde{y}_1, \alpha\varpi\tilde{y}_2)$$

where the variables with tilde are the perturbations from (23), e.g., $\tilde{r} := r - \alpha$, and

$$\begin{aligned}b &= \begin{bmatrix}0 & \gamma c & 0 & 1 & 0\end{bmatrix}/\alpha\\ \Sigma &= \begin{bmatrix}A_1 + \varepsilon B_1 & A_2\\ \varepsilon C_1 & 0\end{bmatrix}, \quad \begin{aligned}s &:= \sin\varpi t,\\ c &:= \cos\varpi t,\end{aligned}\\ \begin{bmatrix}A_1\\ C_1\end{bmatrix} &:= \left[\begin{array}{ccc}-\tilde{\mu} & 0 & 0\\ \tilde{\mu}s & 0 & 1\\ \tilde{\mu}\varpi c & -\varpi^2 & -d\\ \hline 0 & \tilde{\eta}c & 0\\ -\tilde{\kappa} & -\tilde{\kappa}s & 0\end{array}\right],\\ \begin{bmatrix}B_1 & A_2\end{bmatrix} &:= \left[\begin{array}{ccc|cc}0 & \tilde{\gamma}s & 0 & 0 & 0\\ 0 & -\tilde{\gamma} & 0 & -c & 0\\ 0 & 0 & 0 & \varpi s + dc & c\end{array}\right],\end{aligned} \tag{24}$$

Thus, solution (22) is orbitally exponentially stable if and only if the system $\dot{\tilde{\xi}} = \Sigma\tilde{\xi}$ is exponentially stable . We use Lemma 1 to prove the stability. Noting that A_1 is block triangular, it is

easy to see that it is Hurwitz. To show that $\mathcal{B}$ is Hurwitz as well, note that (7) is an exponentially stable linear time-invariant system driven by a sinusoidal input, and the steady state solution is easily obtained as

$$\mathcal{L}_o = \frac{1}{d\varpi}\begin{bmatrix} 0 & 0 \\ -2\varpi c & s \\ * & * \end{bmatrix},$$

where $*$ denotes irrelevant entries. We can then calculate $\mathcal{B}$ as

$$\mathcal{B} = \int_0^T C_1 \mathcal{L}_o dt = -\frac{T}{2}\begin{bmatrix} \tilde{\eta}/d & 0 \\ 0 & \tilde{\kappa}/(\varpi d) \end{bmatrix},$$

which is clearly Hurwitz. ■

Theorem 2 guarantees orbital exponential stability of the natural oscillation when the control gains are sufficiently small, which yields slow adaptation of the estimated parameters. However, the gains can in fact be large for fast adaptation, and may be tuned as follows for practical purposes. First, fix a positive constant γ_o, let $\gamma = \epsilon\gamma_o$ for a positive parameter ϵ, and set η and κ similarly. Starting with a small ϵ, run the closed-loop experiments for gradually increasing values of ϵ and search for the maximum rate of convergence.

If a more systematic approach is preferred, one can perform model-based analysis using estimates of damping $\hat{d}$ and natural frequency $\hat{\varpi}$, obtained for instance from an experiment with a small ϵ. First, calculate the maximum Floquet multiplier, $\lambda_{\rm M}$, for the linear periodic system $\dot{\tilde{\xi}} = \Sigma\tilde{\xi}$ with $(\hat{d}, \hat{\varpi})$ in (24). That is, $\lambda_{\rm M}$ is the eigenvalue of $\Phi(T)$ with the largest magnitude, where $\dot{\Phi} = \Sigma\Phi$, $\Phi(0) = I$, and $T := 2\pi/\hat{\varpi}$. This should yield $|\lambda_{\rm M}| < 1$ for orbital exponential stability when ϵ is small. Increase ϵ and repeat the calculation until $|\lambda_{\rm M}| < 1$ is violated (denote the largest value by $\bar{\epsilon}$). Then an upper bound for $\bar{\varepsilon}$ is given as the smallest of $\bar{\epsilon}\gamma_o$, $\bar{\epsilon}\eta_o$, and $\bar{\epsilon}\kappa_o$. For the control design, one may choose $\epsilon \in (0, \bar{\epsilon})$ that gives the smallest $|\lambda_{\rm M}|$ for the fastest convergence. However, the domain of attraction for the natural oscillation may shrink with increasing ϵ, which would be another consideration for the design. This issue is illustrated by an example in Section VI-B.

V. Extension to Multi-DOF Systems

A. Problem Formulation

In this section, we consider an extension of the result in the previous section to multi-DOF mechanical systems. Let the mechanical system be given by

$$M\ddot{q} + D\dot{q} + Kq = w \tag{25}$$

where $q(t), w(t) \in \mathbb{R}^n$ are generalized coordinates and force inputs, and $M, D, K \in \mathbb{R}^{n\times n}$ are system parameters representing the mass, damping and stiffness. We assume that M, D, and K are positive definite.

Consider a natural mode of oscillation

$$q_d(t) = \alpha \mathsf{e} \sin \varpi t \tag{26}$$

defined by the amplitude parameter $\alpha \in \mathbb{R}$ and a pair of generalized eigenvalue/eigenvector $(\lambda, \mathsf{e}) \in \mathbb{R}^n \times \mathbb{R}$ satisfying

$$(\lambda M - K)\mathsf{e} = 0, \quad \mathsf{e}^{\mathsf{T}} M \mathsf{e} = 1,$$

where $\varpi := \sqrt{\lambda}$ is a natural frequency, and e is the associated mode shape, with the second equation normalizing the magnitude of e. Since M and K are real symmetric positive definite, both e and λ are real, and $\lambda > 0$.

The objective is to achieve entrainment to the arbitrarily chosen mode of natural oscillation in (26) by a nonlinear feedback controller without full knowledge of the mechanical parameters. In particular, we assume that the system parameters are unknown except for e and M. While M can be estimated fairly accurately in practice, the knowledge of e may not be fully justified but is required in the result that follows.

We will formulate a control design problem in the modal coordinates. Define a square matrix $E \in \mathbb{R}^{n\times n}$ so that

$$E := \begin{bmatrix} \mathsf{e} & * \end{bmatrix}, \quad E^{\mathsf{T}} M E = I,$$

where $*$ represents unspecified entries. Then the original system can be transformed into the form

$$\ddot{z} + \nabla\dot{z} + \Lambda z = u, \tag{27}$$

where $z(t) \in \mathbb{R}^n$ are the modal coordinates and

$$q = Ez, \quad w = MEu$$

$$\nabla := E^{\mathsf{T}} D E \quad \Lambda := E^{\mathsf{T}} K E = \mathrm{diag}(\varpi^2, \Omega),$$

The natural oscillation of z corresponding to (26) is

$$z_d(t) = \mathrm{col}(\alpha \sin \varpi t, 0). \tag{28}$$

Now, the problem is reduced to the design of a controller that generates control input u using the sensory information of z.

Our goal is to design a controller that can achieve orbital exponential stability of $z = z_d$. We seek an adaptive controller that meets the objective with no information of the system parameters Δ and Λ. Note that the natural oscillation $z = z_d$ is a solution of (27) if and only if the control input compensates for the damping as

$$u = \nabla \dot{z}_d(t) = \begin{bmatrix} d \\ \delta \end{bmatrix} \alpha\varpi \cos \varpi t,$$

where the partitioned blocks of ∇ are defined by

$$\nabla = \begin{bmatrix} d & \delta^{\mathsf{T}} \\ \delta & \Delta \end{bmatrix}, \qquad \begin{matrix} d \in \mathbb{R}, \quad \delta \in \mathbb{R}^{n-1}, \\ \Delta \in \mathbb{R}^{(n-1)\times(n-1)}. \end{matrix}$$

Since ∇ and Λ are unknown, the controller should be capable of estimating d, δ and ϖ.

The formal problem statement is given as follows.

Problem 3: Let a mechanical system in (27) with positive definite (∇, Λ), and a positive scalar $\alpha \in \mathbb{R}$ be given, and consider the natural oscillation z_d defined in (28). Design a feedback controller of the form

$$\dot{x} = f(x, y, z), \quad \dot{y} = g(x, z), \quad u = h(x, y),$$

where $(x, y) \in \mathbb{R}^n \times \mathbb{R}^m$ is the state vector, to achieve the natural oscillation with amplitude α in the steady state. In particular, the design specifications are the following:

(i) There exists an orbitally exponentially stable solution $(x, y, z, \dot{z})$ of the closed-loop system such that

$$x(t) = x(t + T), \quad y(t) \equiv \mathrm{col}(\varpi, d, \delta), \quad z = z_d.$$

(ii) Functions f, g and h specifying the controller are independent of the system parameters ∇ and Λ.

B. Approach

The idea for the control design is a direct extension of the single-DOF case in the previous section. We propose the following controller as an extension of (21):

$$\begin{bmatrix}\dot{x}_1\\ \dot{x}_2\end{bmatrix} = \begin{bmatrix}\sigma & y_1\\ -y_1 & \sigma\end{bmatrix}\begin{bmatrix}x_1\\ x_2\end{bmatrix} + \gamma\begin{bmatrix}z_1 - x_1\\ 0\end{bmatrix} \tag{29a}$$

$$\dot{y}_1 = \eta x_2(z_1 - x_1) \tag{29b}$$

$$\dot{y}_2 = \kappa(\alpha^2 - z_1^2 - x_2^2) \tag{29c}$$

$$\dot{y}_3 = -\mathcal{K} z_2 x_1, \tag{29d}$$

$$u = \begin{bmatrix}y_2\\ y_3\end{bmatrix} y_1 x_2, \quad \sigma = \mu(\alpha^2 - x_1^2 - x_2^2), \tag{29e}$$

where $\gamma, \eta, \kappa, \mu \in \mathbb{R}$ are positive constants, $\mathcal{K} \in \mathbb{R}^{(n-1)\times(n-1)}$ is a symmetric positive definite matrix, $z_1(t) \in \mathbb{R}$ and $z_2(t) \in \mathbb{R}^{n-1}$ are defined by $z = \mathrm{col}(z_1, z_2)$, and $x_i(t), y_i(t) \in \mathbb{R}$ are scalar variables for $i = 1, 2$ and $y_3(t) \in \mathbb{R}^{n-1}$. Equations (29a)–(29c) and the first entry of u in (29e) are identical to (21a)–(21c) when z_1 is replaced by z. Hence, variables (y_1, y_2) estimate (ϖ, d), and (x_1, x_2) locally converges to the orbit $(\alpha\sin\varpi t, \alpha\cos\varpi t)$, provided $z_2 = 0$. The rationale for the remaining part of the controller is explained below.

The additional variable $y_3(t)$ in (29d) is introduced as an estimate for δ. To see how it works, consider the situation where the trajectory is on the target orbit, i.e. $y_1 = \varpi$, $x_1 = z_1 = \alpha\sin\varpi t$, and $x_2 = \alpha\cos\varpi t$, except for nonzero errors in $y_3 - \delta$ and z_2. The z_2 dynamics can be described as

$$\ddot{z}_2 + \Delta\dot{z}_2 + \Omega z_2 = (y_3 - \delta)\dot{x}_1. \tag{30}$$

If $\|\mathcal{K}\|$ is sufficiently small, y_3 can be regarded as constant and z_2 is a sinusoid. Then the dynamics of $\dot{y}_3$ in (29d) is approximated as

$$\dot{y}_3 \approx -\frac{1}{T}\int_0^T \mathcal{K} z_2 x_1 dt = -\frac{1}{\varpi^2 T}\int_0^T \mathcal{K}\dot{z}_2\dot{x}_1 dt, \tag{31}$$

where the latter equality holds since z_2 and x_1 are sinusoids of frequency ϖ. Multiplying (30) by $\dot{z}_2^{\mathsf{T}}$ from left, taking the average over the cycle, and using (31), we have

$$\begin{aligned} 0 < \int_0^T \dot{z}_2^{\mathsf{T}}\Delta\dot{z}_2 dt &= (y_3 - \delta)^{\mathsf{T}}\int_0^T \dot{z}_2\dot{x}_1 dt \\ &\approx -\varpi^2 T(y_3 - \delta)^{\mathsf{T}}\mathcal{K}^{-1}(\dot{y}_3 - \dot{\delta}) \\ &= -\frac{\varpi^2 T}{2}\frac{d}{dt}\Big(\|\mathcal{K}^{-1/2}(y_3 - \delta)\|^2\Big). \end{aligned}$$

Thus the derivative of $\|\mathcal{K}^{-1/2}(y_3 - \delta)\|$ is negative, making y_3 converge to δ. When $y_3 = \delta$, the second entry of u in (29e) decouples z_2 from z_1, achieving convergence of z_2 to zero due to the inherent stability of the mechanical system.

C. Result

The following theorem gives a sufficient condition for entrainment to the desired natural oscillation.

Theorem 3: Consider mechanical system (27) and the controller given by (29). Suppose ∇ and Λ are symmetric positive definite, and $\alpha, \mu, \gamma, \eta, \kappa \in \mathbb{R}$ are positive constants and $\mathcal{K} \in \mathbb{R}^{(n-1)\times(n-1)}$ is a positive definite matrix. Then

$$\begin{aligned} &\mathrm{col}(z, \dot{z}, x_1, x_2, y_1, y_2, y_3) \\ &= \mathrm{col}(z_d, \dot{z}_d, \alpha\sin\varpi t, \alpha\cos\varpi t, \varpi, d, \delta) \end{aligned} \tag{32}$$

is a solution of the closed-loop system. Moreover, there exists $\bar{\varepsilon} > 0$ such that the solution is orbitally exponentially stable whenever γ, η, κ and $\|\mathcal{K}\|$ are smaller than $\bar{\varepsilon}$.

Proof: The framework for the proof is roughly the same as the single-DOF case, with some additional complication due to the extra degrees of freedom. With the normalized controller parameters

$$\varepsilon\begin{bmatrix}\tilde{\gamma} & \tilde{\eta} & \tilde{\kappa}\end{bmatrix} := \begin{bmatrix}\gamma & \eta\alpha^2 & 2\kappa\alpha^2\varpi\end{bmatrix}, \quad \varepsilon\tilde{\mathcal{K}} := \alpha^2\varpi\mathcal{K}, \quad \tilde{\mu} := 2\mu\alpha^2,$$

we prove orbital exponential stability for the case where $\tilde{\gamma}$, $\tilde{\eta}$, $\tilde{\kappa}$, and $\tilde{\mu}$ are arbitrary positive constants, $\tilde{\mathcal{K}}$ is an arbitrary positive definite matrix, and $\varepsilon > 0$ is sufficiently small. Let us introduce a coordinate transformation and a new state vector (θ, ξ) where

$$\xi := \mathrm{col}(r, e_1, z_2, e_2, \dot{z}_2, \alpha y_1, \alpha\varpi y_2, \alpha\varpi y_3).$$

$$\begin{aligned} x_1 &= r\sin\theta, \quad e_1 = z_1 - x_1, \\ x_2 &= r\cos\theta, \quad e_2 = \dot{z}_1 - \varpi x_2, \end{aligned}$$

The trajectory (32) in the new coordinates is given by

$$\begin{aligned} \theta &= \varpi t \\ \xi &= \mathrm{col}(\alpha, 0, 0, 0, 0, \alpha\varpi, \alpha\varpi d, \alpha\varpi\delta). \end{aligned} \tag{33}$$

Linearization around the solution (33) yields

$$\begin{bmatrix}\dot{\tilde{\theta}}\\ \dot{\tilde{\xi}}\end{bmatrix} = \begin{bmatrix}0 & b\\ 0 & \Sigma\end{bmatrix}\begin{bmatrix}\tilde{\theta}\\ \tilde{\xi}\end{bmatrix},$$

$$\tilde{\xi} = \mathrm{col}(\tilde{r}, e_1, z_2, e_2, \dot{z}_2, \alpha\tilde{y}_1, \alpha\varpi\tilde{y}_2, \alpha\varpi\tilde{y}_3)$$

where the variables with tilde are the perturbations from (33), e.g., $\tilde{y}_1 := y_1 - \varpi$, and

$$b = \begin{bmatrix}0 & \gamma c & 0 & 0 & 0 & 1 & 0 & 0\end{bmatrix}/\alpha$$

$$\Sigma = \begin{bmatrix}A_1 + \varepsilon B_1 & A_2\\ \varepsilon C_1 & 0\end{bmatrix}, \qquad s := \sin\varpi t, \quad c := \cos\varpi t,$$

$$\left[\begin{array}{c}A_1\\ C_1\end{array}\right] := \left[\begin{array}{ccccc} -\tilde{\mu} & 0 & 0 & 0 & 0\\ \tilde{\mu}s & 0 & 0 & 1 & 0\\ 0 & 0 & 0 & 0 & I\\ \tilde{\mu}\varpi c & -\varpi^2 & 0 & -d & -\delta^{\mathsf{T}}\\ 0 & 0 & -\Omega & -\delta & -\Delta \\ \hline 0 & \tilde{\eta}c & 0 & 0 & 0\\ -\tilde{\kappa} & -\tilde{\kappa}s & 0 & 0 & 0\\ 0 & 0 & -\tilde{\mathcal{K}}s & 0 & 0 \end{array}\right],$$

$$\begin{bmatrix}B_1 & A_2\end{bmatrix} := \left[\begin{array}{ccccc|ccc} 0 & \tilde{\gamma}s & 0 & 0 & 0 & 0 & 0 & 0\\ 0 & -\tilde{\gamma} & 0 & 0 & 0 & -c & 0 & 0\\ 0 & 0 & 0 & 0 & 0 & 0 & 0 & 0\\ 0 & 0 & 0 & 0 & 0 & \varpi s + dc & c & 0\\ 0 & 0 & 0 & 0 & 0 & \delta c & 0 & cI \end{array}\right].$$

Thus, solution (32) is orbitally exponentially stable if and only if the system $\dot{\tilde{\xi}} = \Sigma\tilde{\xi}$ is exponentially stable .

From Lemma 1, orbital exponential stability is shown if the dynamics of A_1 and $\mathcal{B}$ are both exponentially stable . First note that $A_1(t)$ has a block-triangular structure with a negative number on the first diagonal entry and the second diagonal block is constant and Hurwitz due to stability of plant (27). Thus the linear periodic system with $A_1(t)$ is exponentially stable. Next note that the periodic solution to (7) has the form

$$\mathcal{L}_o = \begin{bmatrix} 0 \\ M_1 \\ M_2 \end{bmatrix} s + \begin{bmatrix} 0 \\ N_1 \\ N_2 \end{bmatrix} c. \tag{34}$$

Let A_2 and C_1 be expressed as

$$A_2 = \begin{bmatrix} 0 \\ Q_1 c \\ Q_2 c + Q_3 s \end{bmatrix}, \quad C_1 = \begin{bmatrix} R_1 & R_2 s + R_3 c & 0 \end{bmatrix},$$

with appropriate coefficients Q_i and R_i. Substituting (34) into (7), setting the coefficients of s and c to zero, and eliminating M_2 and N_2, we obtain

$$\begin{bmatrix} M_1 \\ N_1 \end{bmatrix} = V^{-1}W,$$

where

$$V := \begin{bmatrix} \varpi\nabla & \Lambda - \varpi^2 I \\ \varpi^2 I - \Lambda & \varpi\nabla \end{bmatrix}, \quad W := \begin{bmatrix} \nabla Q_1 + Q_2 \\ \varpi Q_1 - Q_3 \end{bmatrix}.$$

Here, we noted that V is invertible because $V + V^\intercal > 0$ due to $\nabla > 0$. Then we can calculate $\mathcal{B}$ as

$$\mathcal{B} = \int_0^T C_1 \mathcal{L}_o dt = \frac{T}{2} \cdot UV^{-1}W, \quad U := \begin{bmatrix} R_2 & R_3 \end{bmatrix}.$$

We first show that $\mathcal{B}$ is nonsingular. Suppose, for contradiction, that there exists a nonzero vector v in the null space of $\mathcal{B}$. Then, defining $w := V^{-1}Wv$, we have

$$UV^{-1}Wv = 0 \quad \Rightarrow \quad Uw = 0, \quad Vw = Wv.$$

Since the left $(n+1)\times(n+1)$ block of U is square nonsingular and the remaining columns are zero, w has the form $w = \mathrm{col}(0, w_2)$ with $w_2 \in \mathbb{R}^{n-1}$. The lower $n-1$ rows of $Vw = Wv$ then gives $\nabla w_2 = 0$, implying $w = 0$ and $Wv = 0$. Since W has full column rank, we conclude $v = 0$. By contradiction, $\mathcal{B}$ must be nonsingular.

An arbitrary eigenvalue λ of $(2/T)\mathcal{B}$ is nonzero and satisfies the characteristic equation

$$\det V \det(\lambda I - UV^{-1}W) = \det(\lambda V - WU) = 0,$$

where we used determinant formulas. Noting that

$$WU = \mathrm{diag}(\tilde{\kappa}, \tilde{\mathcal{K}}, 2\varpi\tilde{\eta}, 0) \geq 0,$$

it follows from Lemma 6 that the real part of $\lambda \in \mathbb{C}$ is negative. Thus $\mathcal{B}$ is Hurwitz and we conclude the result. ∎

In Theorem 3, the controller is independent of the plant parameters except for the mode shape e and the mass matrix M. The proof reveals that stability of the plant (27) ensures the convergence of the synchronization error e_2 and the unselected natural modes z_2, which can therefore be made faster by an additional minor feedback that modifies Λ and Ω. Convergence of the adaptation variables may be made faster through the Floquet analysis as in the single-DOF case.

VI. Numerical Examples

A. Adaptive Oscillator

This section illustrates how our adaptive oscillator works, in comparison with the one presented in [32]. The former is given by (17) and its convergence property is guaranteed as in Theorem 1. The latter is given by an Andronov-Hopf oscillator with a Hebbian learning mechanism:

$$\begin{bmatrix} \dot{x}_1 \\ \dot{x}_2 \end{bmatrix} = \begin{bmatrix} 1 - r^2 & \omega_{\mathrm{est}} \\ -\omega_{\mathrm{est}} & 1 - r^2 \end{bmatrix} \begin{bmatrix} x_1 \\ x_2 \end{bmatrix} + \varepsilon \begin{bmatrix} 0 \\ z \end{bmatrix} \tag{35a}$$

$$\dot{\omega}_{\mathrm{est}} = -\varepsilon z x_1 / \sqrt{r}, \quad r := x_1^2 + x_2^2, \tag{35b}$$

and it was explained using perturbation argument [32] that ω_{est} globally (and approximately) converges to a frequency component of periodic input z when parameter $\varepsilon > 0$ is small. The dynamic Hebbian learning is a general heuristic method that applies to other oscillators and non-sinusoidal signals.

For the numerical study, we use the input $z(t) = \cos(30t)$ for both oscillators. The system parameters and initial states are set as

$$\mu = 1, \quad \gamma = 10, \quad \eta = 50, \quad \kappa = 2,$$
$$x(0) = \mathrm{col}(0, 1), \quad y(0) = \mathrm{col}(40, 2),$$

for our adaptive oscillator (17) and

$$\varepsilon = 0.4, \quad 0.6, \quad 0.8, \quad 1, \quad \text{or} \quad 100,$$
$$x(0) = \mathrm{col}(0, 1), \quad \omega_{\mathrm{est}}(0) = 40,$$

for the Hebbian learning oscillator (35). The input z and initial states are taken from [32] and are used for both here, except that the initial estimate of the amplitude $y_2(0)$ is needed for (17) and is set twice as large as the true value.

Figure 1 shows the input z and response x_1, as well as the estimated frequency y_1 and amplitude y_2, for the adaptive oscillator in (17). We see that x_1 synchronizes with z within several cycles, while the estimated frequency and amplitude converge to their true values. For comparison, Fig. 2 shows the estimated frequency using the Hebbian learning approach in [32]. For small values of ε, the learning process takes a long time as seen in Fig. 2 (top), which is reproduced from the ε values in [32]. With a larger value of ε, their method could achieve faster convergence as seen in Fig. 2 (bottom), but there is a trade-off between convergence rate and steady-state error. The larger the parameter ε, the faster the convergence, but the larger the error in the steady state. In contrast, such trade-off does not exist in our method since the adaptation mechanism is designed so that the error is zero at convergence.

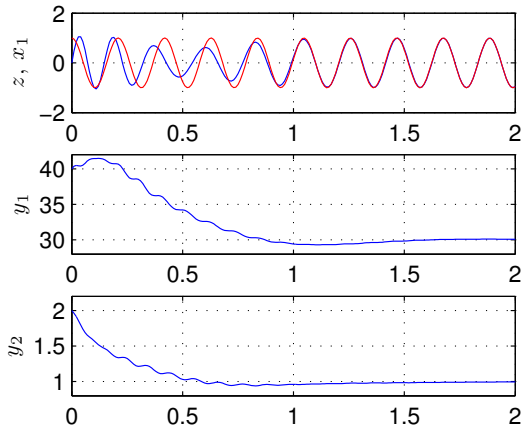

Fig. 1. Adaptive Andronov-Hopf Oscillator

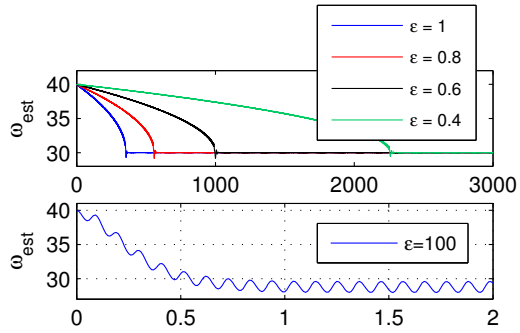

Fig. 2. Andronov-Hopf Oscillator with Hebbian Learning

B. Single-DOF Natural Entrainment

We now present an example of feedback control for natural entrainment. Consider the single-DOF mechanical system in (19) with parameter values switching from one set to another:

$$\begin{aligned}(m,d,k) &= (1,2,16) \quad \text{when } t<20,\\ &= (1,5,4) \quad \text{when } t\geq 20.\end{aligned} \tag{36}$$

Note that the frequency of natural oscillation $z_n(t)$ in (20) is switched from $\varpi = 4$ to 2. We design a feedback controller in (21) so that the frequency of mechanical oscillation is automatically tuned into the current natural frequency. The desired oscillation amplitude is fixed as $\alpha = 1$ at all time. The controller parameters are set as

$$\mu = 2, \quad \eta = 3\epsilon, \quad \kappa = \epsilon, \quad \gamma = 2\epsilon.$$

Figure 4 shows the magnitude of the maximum Floquet multiplier $|\lambda_{\rm M}|$ as a function of ϵ, for the linear periodic system in (24) with $(\varpi, d) = (4, 2)$. The curve takes the value $|\lambda_{\rm M}| = 1$ at $\epsilon = 0$ with a negative slope so that $|\lambda_{\rm M}|$ is less than 1 for sufficiently small $\epsilon > 0$, as guaranteed by Theorem 2. As shown, $|\lambda_{\rm M}|$ remains less than 1 for larger values of ϵ, which can be optimized to achieve the smallest $|\lambda_{\rm M}|$ (indicated by the star) for the fastest convergence.

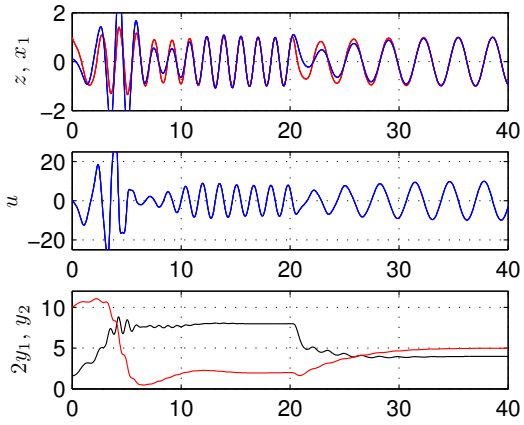

Fig. 3. AHO Controller with single-DOF system. Top row: z (blue), x_1 (red). Bottom row: $2y_1$ (black), y_2 (red).

The closed-loop system is simulated for the case $\epsilon = 1$ with the following initial conditions. For the controller state,

$$x(0) = \frac{\alpha x_o}{\|x_o\|}, \quad x_o := \begin{bmatrix} z(0) \\ \dot{z}(0)/\omega_o \end{bmatrix}, \quad y(0) = \begin{bmatrix} \omega_o \\ d_o \end{bmatrix}, \tag{37}$$

where (ω_o, d_o) are the initial estimates for the natural frequency and damping. The choice of $x(0)$ is made so that the initial state would be exactly on the target orbit if the plant state $(z(0), \dot{z}(0))$ were on the natural oscillation orbit and the frequency/damping estimates (ω_o, d_o) were correct.

Figure 3 shows the simulation result, where the initial plant state is ten-fold away from the target natural oscillation in magnitude ($z(0) = 0.1$ and $\dot{z}(0) = 0$), and the initial estimates for (ϖ, d) are five times smaller/larger than the correct values, $(\omega_o, d_o) = (4/5, 2 \times 5)$. The mechanical variable $z(t)$ eventually synchronizes with x_1 in the steady state, and both of them converge to a sinusoidal signal with the natural frequency ϖ and the prescribed amplitude $\alpha = 1$. Furthermore, estimated natural frequency y_1 and damping y_2 converge to the true values ϖ and d, respectively.

To examine the domain of attraction, the closed-loop system is simulated for the plant $(m, d, k) = (1, 2, 16)$ and the AHO controller designed above with $\epsilon = 1$. The initial state is set by choosing a point in the plant state space $(z, \dot{z})$ and specifying the controller state accordingly as in (37) with $(\omega_o, d_o) = (4/5, 2 \times 5)$. If z and x_1 converge to the natural oscillation, then the initial state is deemed within the domain of attraction. Repeating the simulations for various values

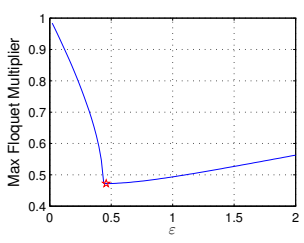

Fig. 4. Maximum Floquet multiplier

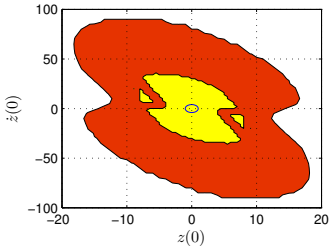

Fig. 5. Domain of attraction

of the initial plant state, the cross section of the domain of attraction can be visualized as a region in the $(z, \dot{z})$ plane. The result is shown as the yellow region in Fig. 5. We see that the region is fairly large in comparison with the target orbit of the natural oscillation indicated by the tiny blue ellipse near the origin. Hence, the trajectory would converge back to the target orbit after a practically possible perturbation due to a disturbance, by resetting $x(0)$ as in (37). If desired, the domain of attraction can be further enlarged at the expense of slower adaptation by choosing a smaller value of ϵ. For example, the red region is generated for $\epsilon = 0.1$.

For comparison, we consider the passivity based adaptive controller (PBAC) in Section 11.3.4 of [44], which gives

$$\begin{aligned} u &= \hat{m}a + \hat{d}v + \hat{k}z - c_1 r, & r &:= \dot{z} - v, \\ \dot{\hat{m}} &= -c_3 a r, & v &:= \dot{z}_{\rm ref} - c_2 e, \\ \dot{\hat{d}} &= -c_4 v r, & e &:= z - z_{\rm ref}, \\ \dot{\hat{k}} &= -c_5 z r, & a &:= \ddot{z}_{\rm ref} - c_2 \dot{e}, \end{aligned}$$

where $z_{\rm ref}$ is a given reference command. The controller estimates the unknown plant parameters by $(\hat{m}, \hat{d}, \hat{k})$ and tune the control gains to track $z_{\rm ref}$ by z asymptotically. To achieve the natural oscillation, the natural frequency ϖ has to be somehow estimated in advance. Assuming this is done, the reference is set as $z_{\rm ref}(t) := \sin(\varpi t)$. For an example design, we consider the same simulation condition as in the previous AHO case with the switching plant in (36). With $\varpi = 4$ for the reference $z_{\rm ref}$, we aim for the natural oscillation before the plant switching at $t = 20$. The controller parameters are tuned through closed-loop simulations under the initial condition $\hat{d}(0) = d_o$, $\hat{k}(0) = \hat{m}(0)\omega_o^2$, and $\hat{m}(0) = 1$. The result is shown in Fig. 6 for the case

$$c_1 = c_2 = 1, \quad c_3 = 50, \quad c_4 = 5, \quad c_5 = 10.$$

The controller makes z converge to $z_{\rm ref}$ although the estimates $(\hat{m}, \hat{k})$ do not converge to the true values. The tracking $z \to z_{\rm ref}$ is enforced even after the plant dynamics are changed at $t = 20$ as intended by the design, making z deviate away from the natural oscillation of the new dynamics. Such robust tracking may be desired in some applications, but adaptive tracking of the natural oscillation as in Fig. 3 may be preferred in other applications, where the z oscillation of the same amplitude is achieved with a smaller amplitude of input u.

For entrainment to the natural oscillation, the reference command may be adaptively changed as $z_{\rm ref}(t) = \sin(\hat{\varpi} t)$ with $\hat{\varpi} := (\hat{k}/\hat{m})^{1/2}$. This heuristic approach may work to some extent, but there are difficulties. First of all, convergence to the natural oscillation is not theoretically guaranteed. Moreover, the controller requires state measurements, the dynamics have a singularity at $\hat{m} = 0$, and the estimate $\hat{\varpi}$ may become undefined on the trajectory when $\hat{k}/\hat{m}$ becomes negative (observe that $\hat{m}(t)$ in Fig. 6 does go across the origin). Hence, it would require a substantial development beyond the existing PBAC technique if adaptive natural entrainment is desired with output feedback. The AHO control avoids all these difficulties.

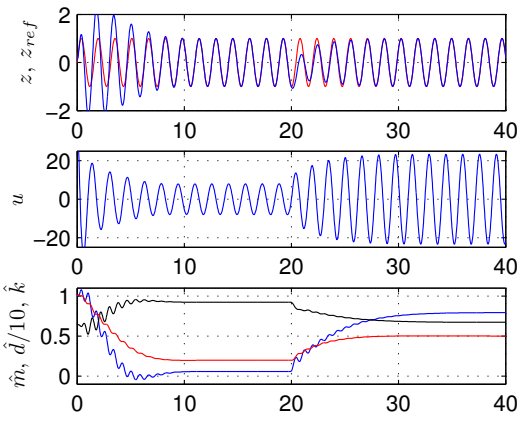

Fig. 6. Passivity based adaptive controller with single-DOF system. Top row: z (blue), $z_{\rm ref}$ (red). Bottom row: $\hat{m}$ (blue), $\hat{d}/10$ (red), $\hat{k}$ (black).

C. Multi-DOF Natural Entrainment

Consider a triple (three-link) pendulum in a gravity field with the first link fixed to the inertial frame through a rotational joint. The $i^{\rm th}$ link has mass m_i and length ℓ_i, and the $i^{\rm th}$ joint has friction with damping coefficient d_i and an actuator to create torque input u_i. The equation of motion is given by

$$J_q \ddot{q} + G_q \dot{q}^2 + D\dot{q} + K \sin(q) = Bu, \tag{38}$$

where q_i is the angular displacement of the $i^{\rm th}$ link, $\dot{q}^2$ is the vector whose $i^{\rm th}$ entry is $\dot{q}_i^2$, and

$$\begin{aligned} &J_q := J_o + S_q Q S_q + C_q Q C_q, \quad G_q := S_q Q C_q - C_q Q S_q, \\ &Q := L^{\mathsf{T}} M L, \quad K := \mathrm{diag}(L^{\mathsf{T}} M \mathbf{1}) g, \quad D := B D_o B^{\mathsf{T}}, \\ &M := \mathrm{diag}(m_1, m_2, m_3), \quad J_o := \mathrm{diag}\left(m_1\ell_1^2, m_2\ell_2^2, m_3\ell_3^2\right)/12, \\ &S_q := \mathrm{diag}(\sin q_1, \sin q_2, \sin q_3), \quad D_o = \mathrm{diag}(d_1, d_2, d_3), \\ &C_q := \mathrm{diag}(\cos q_1, \cos q_2, \cos q_3), \quad \mathbf{1} := \mathrm{col}(1,1,1), \\ &B := \begin{bmatrix} 1 & -1 & 0 \\ 0 & 1 & -1 \\ 0 & 0 & 1 \end{bmatrix}, \quad L := \begin{bmatrix} \ell_1/2 & 0 & 0 \\ \ell_1 & \ell_2/2 & 0 \\ \ell_1 & \ell_2 & \ell_3/2 \end{bmatrix}. \end{aligned}$$

We use the following parameter values:

$$\ell_i = 1, \quad m_i = 1, \quad d_i = 5, \quad g = 9.81,$$

for $i = 1, 2, 3$. The linearization around the origin gives a linear system of the form (25), which can be transformed into the modal form (27) with

$$E = \begin{bmatrix} 0.273 & -0.655 & -1.06 \\ 0.361 & 0 & 2.06 \\ 0.454 & 1.96 & -1.76 \end{bmatrix}, \quad \Lambda = \begin{bmatrix} \varpi_1^2 & 0 & 0 \\ 0 & \varpi_2^2 & 0 \\ 0 & 0 & \varpi_3^2 \end{bmatrix},$$

$$\nabla = \begin{bmatrix} 0.454 & 0.311 & -1.83 \\ 0.311 & 23.6 & -23.9 \\ -1.83 & -23.9 & 127 \end{bmatrix}, \quad \begin{bmatrix} \varpi_1 \\ \varpi_2 \\ \varpi_3 \end{bmatrix} = \begin{bmatrix} 2.18 \\ 5.42 \\ 10.2 \end{bmatrix},$$

where E is the normalized modal matrix. The $i^{\rm th}$ natural mode of oscillation is given by $q(t) = \alpha_i \mathbf{e}_i \sin(\varpi_i t)$ where $\mathbf{e}_i \in \mathbb{R}^3$ is the $i^{\rm th}$ column of E and $\alpha_i \in \mathbb{R}$ is an amplitude parameter.

To achieve entrainment to the natural oscillations, we used Theorem 3 and designed two controllers (29) with $\mathcal{K} =$

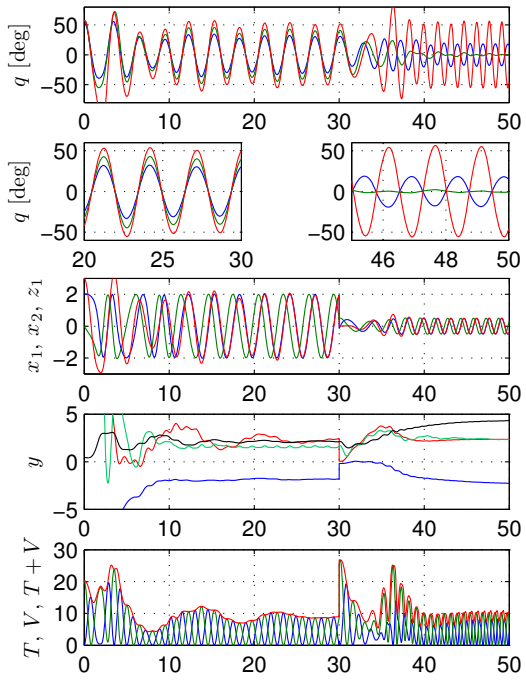

Fig. 7. Closed-loop simulation with multi-DOF AHO Controller.

$\mathrm{diag}(k_1, k_2)$ and

$$(\alpha, \mu, \gamma, \eta, \kappa, k_1, k_2) = \begin{cases} (20, 1, 1, 5, 2, 200, 100)/10, \\ (5, 5, 5, 100, 500, 2000, 10)/10 \end{cases}$$

for the first and second modes, respectively. The parameter α is set so that the maximum amplitude of the link angle is around 50^o, and the other parameters are tuned so that (x, y) converges within several cycles of oscillations (the larger the parameter, the faster the convergence).

The closed-loop system of the original nonlinear plant (38) and controller (29) is simulated under the following condition. The controller for the first mode is used for $0 \le t \le 30$, then switched to the one for the second mode for $30 \le t \le 50$. The initial state for the plant is set to $q(0) = \mathrm{col}(1, 1, 1)$ and $\dot{q}(0) = 0$, and that for the controller is set by (37) with $\alpha = 2$, $(\omega_o, d_o) = (\varpi_1/5, 5E^{\mathsf{T}}De_1)$, $\dot{z}(0) = 0$, and $z(0)$ being the first entry of $E^{-1}q(0)$. When the controller is switched at $t = 30$, its state x was reset in accordance with (37) while y was kept unchanged.

Figure 7 shows the simulation result. The top two rows indicate that the plant state converges to oscillations with mode shapes similar to the first and second modes of natural oscillations. The third row shows convergence of the AHO state x with the prescribed amplitude α, and its synchronization with the plant state z_1 (red). The fourth row plots the estimated plant parameters $(\hat{\varpi}, \hat{d}, \hat{\delta}) := y$ in the controller, where the (black,red,blue,green) curves correspond to $(\hat{\varpi}, 5\hat{d}, \hat{\delta}_1, 5\hat{\delta}_2)$ before $t = 30$ and $(\hat{\varpi}, \hat{d}/10, \hat{\delta}_1/10, 5\hat{\delta}_2)$ after $t = 30$ (the scaling factors are introduced to fit the curves within a common frame). While the damping parameters are (approximately) converging to the correct values in ∇, the frequency estimate converges to smaller values than ϖ_i, especially for the second mode ($\hat{\varpi}_1 = 2.12$ and $\hat{\varpi}_2 = 4.38$). This may correspond to the fact that the natural frequencies ϖ_i from the linearized model are larger than those for large-amplitude natural oscillations of the original nonlinear system. To verify this, the last row of the figure plots the kinetic energy $T := \dot{q}^{\mathsf{T}} J_q \dot{q}/2$ (blue), the potential energy $V := \mathbf{1}^{\mathsf{T}} K(I - C_q)\mathbf{1}$ (green), and their sum $T + V$ (red), where the quantities are magnified by factor 3 after $t = 30$ for better visibility. The total energy $T + V$ converges approximately to constants toward $t = 30$ and 50, and thus is preserved in the steady state as it should be under a natural oscillation.

VII. Conclusion

We have considered a class of perturbed nonlinear systems with slow and fast dynamics, and proposed an approach to analyze orbital exponential stability of a periodic solution through a Floquet analysis with averaging. Based on this framework, we have formulated and solved problems of designing adaptive oscillators using the structure of the Andronov-Hopf oscillator (AHO) for multiple goals. We started with developing an adaptive oscillator that synchronizes with an external periodic signal and explicitly estimates the amplitude and frequency of the signal. We then proposed a method for designing a feedback controller to embed an orbitally exponentially stable limit cycle in the closed-loop system, on which a natural mode of oscillations is achieved for multi-DOF systems. These design results have illustrated benefits of the general framework for the case of uncertain linear mechanical systems. Moreover, numerical examples demonstrated that the proposed design methods were effective also for nonlinear mechanical systems with fast and smooth convergence.

We have focused on stabilization of an unknown natural oscillation of mechanical systems by estimating the relevant system parameters (damping and natural frequency) through an adaptation mechanism. An interesting extension of the current method would be stabilization of an unknown equilibrium point that may vary with system parameters. Such problems arise for instance in deployment of tensegrity structures [45]. The framework in Section II may be useful also for such problems. In fact, the stability analysis result in Lemma 1 directly applies to the system obtained through linearization around an equilibrium, where all the coefficient matrices are constant. The proposed control architecture may remain valid, with modified interpretations of the dynamic components as an adaptive observer. The details are left for further research.

Appendix

Here we provide several lemmas that are used for the developments in this paper. The notation $\|\cdot\|$ is used to mean the spectral norm for a matrix and the Euclidean norm for a vector, when the argument is constant. If the argument is a function of time, it denotes the supremum norm, i.e.,

$$\|A\| = \sup_{t \ge 0} \|A(t)\|.$$

for a time-varying matrix $A(t)$.

Lemma 2: Let matrices $A \in \mathbb{R}^{n\times m}$ and $X_1, X_2 \in \mathbb{R}^{m\times n}$ be given. Suppose $\|A\| \le \alpha$ and $\|X_i\| \le \beta$ with $i = 1, 2$ for positive scalars $\alpha, \beta \in \mathbb{R}$. Then

$$\|X_1AX_1 - X_2AX_2\| \le 4\alpha\beta\|X_1 - X_2\|.$$

Proof:

$$\begin{aligned}
&\|X_1AX_1 - X_2AX_2\| \\
&= \|(X_1 - X_2)AX_2 + X_2A(X_1 - X_2) + (X_1 - X_2)A(X_1 - X_2)\| \\
&\le \|X_1 - X_2\|\alpha\beta + \alpha\beta\|X_1 - X_2\| + \|X_1 - X_2\|\alpha\|X_1 - X_2\| \\
&\le 2\alpha\beta\|X_1 - X_2\| + (\|X_1\| + \|X_2\|)\alpha\|X_1 - X_2\| \\
&= 4\alpha\beta\|X_1 - X_2\|.
\end{aligned}$$

■

Lemma 3 (Boundedness): Let $A_i(t)$, $B_i(t)$, and $C_i(t)$ with $i = 1, 2$ be matrix-valued functions of $t \in \mathbb{R}$ that are continuous and bounded on $t \ge 0$. Suppose the system

$$\dot{x} = A_1(t)x \tag{39}$$

is exponentially stable . Let $\mathcal{L}_o(t)$ be a solution of (7). For each $\varepsilon > 0$, let $\mathcal{L}_\varepsilon(t)$ be the solution to (4) with initial condition $\mathcal{L}_\varepsilon(0) = \mathcal{L}_o(0)$. Then, $\mathcal{L}_o(t)$ is bounded and there exists a positive scalar $\bar{\varepsilon} \in \mathbb{R}$ such that, for each $\varepsilon \in (0, \bar{\varepsilon})$, the function $\mathcal{L}_\varepsilon(t)$ is continuously differentiable and bounded on $t \ge 0$.

Proof: Let $\Psi(t, t_0)$ be the state transition matrix of (39). Then there exist positive scalars $K, a \in \mathbb{R}$ such that

$$\|\Psi(t, \tau)\| \le Ke^{-a(t-\tau)} \tag{40}$$

due to exponential stability of (39), and $\mathcal{L}_o$ can be written as

$$\mathcal{L}_o(t) = \Psi(t, 0)\mathcal{L}_o(0) + \int_0^t \Psi(t, \tau)A_2(\tau)d\tau. \tag{41}$$

Note that $\mathcal{L}_o$ is bounded on $t \ge 0$ because

$$\begin{aligned}
\|\mathcal{L}_o(t)\| &\le \|\Psi(t, 0)\| \cdot \|\mathcal{L}_o(0)\| + \int_0^t \|\Psi(t, \tau)\| \cdot \|A_2(\tau)\|d\tau \\
&\le Ke^{-at}\|\mathcal{L}_o(0)\| + \int_0^t Ke^{-a(t-\tau)}\|A_2(\tau)\|d\tau \\
&\le Ke^{-at}\|\mathcal{L}_o(0)\| + \frac{K}{a}(1 - e^{-at})\|A_2\| \\
&\le K\|\mathcal{L}_o(0)\| + \frac{K}{a}\|A_2\|.
\end{aligned} \tag{42}$$

Continuous differentiability of $\mathcal{L}_\varepsilon(t)$ follows from its definition and continuity of the system matrices. To show the boundedness of $\mathcal{L}_\varepsilon(t)$, let us define $\Delta_\varepsilon(t)$ by (9). Note that $\Delta_\varepsilon(t)$ is the solution of

$$\dot{\Delta}_\varepsilon(t) = A_1(t)\Delta_\varepsilon(t) + G(t, \mathcal{L}_o(t) + \varepsilon\Delta_\varepsilon(t)) \tag{43}$$

with initial condition $\Delta_\varepsilon(0) = 0$, which can be verified by subtracting (7) from (4) and dividing by ε. This Δ_ε can be seen as a fixed point of mapping M defined by

$$M(Y)(t) = \int_0^t \Psi(t, \tau)G(\tau, \mathcal{L}_o(\tau) + \varepsilon Y(\tau))d\tau.$$

We will show that there exists a constant $c > 0$ such that, when $\varepsilon > 0$ is sufficiently small, M is a contraction mapping on

$$\mathbb{B}_o := \{\ Y \in \mathbb{B} : \|Y\| \le c\ \}, \tag{44}$$

where $\mathbb{B}$ is the Banach space of continuous and bounded matrix-valued functions, defined on $t \in [0, \infty)$, and equipped with the supremum norm. Then Δ_ε is the unique fixed point satisfying

$$\Delta_\varepsilon = M(\Delta_\varepsilon), \quad \Delta_\varepsilon \in \mathbb{B}_o$$

and the boundedness of Δ_ε implies that of $\mathcal{L}_\varepsilon$ from (9).

To this end, use (40), go through calculations like (42), and bound G in (5) by the triangle inequality to obtain

$$\|M(Y)\| \le \rho(\|\mathcal{L}_o + \varepsilon Y\|) \tag{45}$$

where ρ is defined by

$$\rho(x) := \frac{K}{a}\Big(\|B_2\| + \big(\|B_1\| + \|C_2\|\big)x + \|C_1\|x^2\Big).$$

Let c be chosen such that $c > \rho(\|\mathcal{L}_o\|)$. Then for sufficiently small $\varepsilon > 0$ and arbitrary $Y \in \mathbb{B}_o$, we have

$$\rho(\|\mathcal{L}_o + \varepsilon Y\|) \le \rho(\|\mathcal{L}_o\| + \varepsilon c) \le c$$

where the first inequality holds since $\rho(x)$ is increasing on $x > 0$. Thus, for such small ε, we have $M(Y) \in \mathbb{B}_o$ whenever $Y \in \mathbb{B}_o$. Finally, for $Y_1, Y_2 \in \mathbb{B}_o$, another inequality can be derived with the help of Lemma 2 as

$$\|M(Y_1) - M(Y_2)\| \le \varepsilon(a + b\varepsilon) \cdot \|Y_1 - Y_2\|,$$

where $a, b \in \mathbb{R}$ are positive constants that depend on the norms of the system matrices and $\mathcal{L}_o$. Hence, for sufficiently small $\varepsilon > 0$, M is a contraction operator on $\mathbb{B}_o$. ■

Lemma 4: Consider the system

$$\dot{x} = \Big(A(t) + M(t)\Big)x.$$

Suppose the system is exponentially stable when $M(t) \equiv 0$. Then there exists $\varepsilon > 0$ such that the system is exponentially stable for all $M(t)$ such that $\|M\| < \varepsilon$.

Proof: See Theorem 1 on p.205 of [42]. ■

Lemma 5: Consider the system

$$\dot{x} = A_\varepsilon(t)x, \quad A_\varepsilon(t) := \varepsilon\Big(A(t) + \varepsilon M_\varepsilon(t)\Big) \tag{46}$$

with $\varepsilon \in \mathbb{R}$, where $A(t)$ is continuous and T-periodic, and $M_\varepsilon(t)$ is bounded for all $t \ge 0$ and $\varepsilon \in (0, \bar{\varepsilon}_1)$ with a given positive scalar $\bar{\varepsilon}_1$. Suppose the matrix

$$\mathfrak{B} := \int_0^T A(t)dt \tag{47}$$

is Hurwitz. Then there exists $\bar{\varepsilon}_2 > 0$ such that system (46) is exponentially stable for all $\varepsilon \in (0, \bar{\varepsilon}_2)$.

Proof: Based on the Peano-Baker series, the state transition matrix of system (46) can be written as

$$\Psi(t, \tau) = I + \int_\tau^t A_\varepsilon(\sigma)d\sigma + \sum_{k=1}^{\infty} \Psi_k(t, \tau),$$

$$\Psi_k(t, \tau) := \int_\tau^t A_\varepsilon(\sigma_1) \cdots \int_\tau^{\sigma_k} A_\varepsilon(\sigma_{k+1})d\sigma_{k+1} \cdots d\sigma_1.$$

Setting $t = \tau + T$, we have

$$\Psi(\tau + T, \tau) = I + \varepsilon\mathfrak{B} + \varepsilon^2\mathfrak{C}_\varepsilon(\tau),$$

$$\mathfrak{C}_\varepsilon(\tau) := \frac{1}{\varepsilon^2}\sum_{k=1}^{\infty} \Psi_k(\tau + T, \tau) + \int_\tau^{\tau+T} M_\varepsilon(\sigma_1)d\sigma_1,$$

Let H and P be matrices such that

$$H = P^{1/2}, \quad P = P^\mathsf{T} > 0, \quad P\mathfrak{B} + \mathfrak{B}^\mathsf{T} P < 0$$

and define

$$\hat{\Psi}(\tau) := H\Psi(\tau + T, \tau)H^{-1}, \quad \hat{\mathfrak{B}} := H\mathfrak{B}H^{-1}.$$

Then we have

$$\hat{\Psi}(\tau)^\mathsf{T}\hat{\Psi}(\tau) = I + \varepsilon(\hat{\mathfrak{B}} + \hat{\mathfrak{B}}^\mathsf{T}) + \varepsilon^2\mathfrak{D}_\varepsilon(\tau) \tag{48}$$

where $\mathfrak{D}_\varepsilon(\tau)$ is a quadratic function of $\mathfrak{B}$ and $\mathfrak{C}_\varepsilon(\tau)$. Now, let $a, m \in \mathbb{R}$ be positive scalars such that

$$\|A_\varepsilon\| \le a\varepsilon, \quad \|M_\varepsilon\| \le m, \quad \forall\ \varepsilon \in (0, \bar{\varepsilon}_1),$$

and define $\bar{\varepsilon}_3 := \min(1/(aT), \bar{\varepsilon}_1)$. Then, for $\varepsilon \in (0, \bar{\varepsilon}_3)$,

$$\|\mathfrak{C}_\varepsilon\| \le \frac{1}{\varepsilon^2}\sum_{k=1}^{\infty}(aT\varepsilon)^{k+1} + mT = \frac{(aT)^2}{1 - aT\varepsilon} + mT$$

which implies $\|\mathfrak{D}_\varepsilon\| < d$ for some constant $d \in \mathbb{R}$ independent of ε. Note that the eigenvalues of $\hat{\mathfrak{B}} + \hat{\mathfrak{B}}^\mathsf{T}$ are all real negative by construction, and denote the maximum and minimum by $-\lambda_M$ and $-\lambda_m$, respectively. Then, from (48),

$$\|\hat{\Psi}\|^2 \le 1 - \varepsilon\lambda_M + \varepsilon^2 d$$

for all $\varepsilon \in (0, \bar{\varepsilon}_4)$ where $\bar{\varepsilon}_4$ is the smaller of $\bar{\varepsilon}_3$ and $1/\lambda_m$. We now see that there exists $\bar{\varepsilon}_2 > 0$ such that $\|\hat{\Psi}\| < 1$ for $\varepsilon \in (0, \bar{\varepsilon}_2)$. Finally, for arbitrary $t_o \ge 0$ and positive integer n, we have

$$\Psi(t_n, t_o) = H^{-1}\left(\prod_{k=1}^{n}\hat{\Psi}(\tau_k)\right)H,$$
$$t_n := t_o + nT, \quad \tau_k := t_o + (k-1)T,$$

and hence $\|\Psi(t_n, t_o)\|$ converges to zero as $n \to \infty$, provided $\varepsilon \in (0, \bar{\varepsilon}_2)$, proving exponential stability of (46). ■

Lemma 6: Let $n \times n$ real matrices M and K be given. Suppose $M + M^\mathsf{T} > 0$ and $K = K^\mathsf{T} \ge 0$. Let $\lambda \in \mathbb{C}$ be a nonzero generalized eigenvalue satisfying

$$\det(\lambda M + K) = 0.$$

Then the real part of λ is negative.

Proof: Let M be expressed as $M = P + S$ with symmetric P and skew symmetric S. By definition, there exists a nonzero vector $v \in \mathbb{C}^n$ such that

$$\big(\lambda(P + S) + K\big)v = 0.$$

Let

$$p := v^*Pv > 0, \quad q := v^*Kv \ge 0, \quad j\omega := v^*Sv,$$

where we noted that the first two are real positive and nonnegative since $M + M^\mathsf{T}$ and K are symmetric positive (semi)definite, and the last term is purely imaginary since S is skew symmetric. Then

$$v^*\big(\lambda(P + S) + K\big)v = \lambda(p + j\omega) + q = 0$$
$$\Rightarrow \quad \lambda = -\frac{q}{p + j\omega} \quad \Rightarrow \quad \Re[\lambda] = -\frac{pq}{p^2 + \omega^2} < 0,$$

where q is positive since λ is nonzero. ■

REFERENCES

[1] Y. Sakagami, R. Watanabe, C. Aoyama, S. Matsunaga, N. Higaki, and K. Fujimura, "The intelligent asimo: System overview and integration," in *Intelligent Robots and Systems, 2002. IEEE/RSJ International Conference on*, vol. 3, pp. 2478–2483, IEEE, 2002.

[2] R. Tajima, D. Honda, and K. Suga, "Fast running experiments involving a humanoid robot," in *Robotics and Automation, 2009. ICRA'09. IEEE International Conference on*, pp. 1571–1576, IEEE, 2009.

[3] H. Kazerooni, J.-L. Racine, L. Huang, and R. Steger, "On the control of the berkeley lower extremity exoskeleton (bleex)," in *Robotics and automation, 2005. ICRA 2005. Proceedings of the 2005 IEEE international conference on*, pp. 4353–4360, IEEE, 2005.

[4] A. M. Oymagil, J. K. Hitt, T. Sugar, and J. Fleeger, "Control of a regenerative braking powered ankle foot orthosis," in *Rehabilitation robotics, 2007. ICORR 2007. IEEE 10th international conference on*, pp. 28–34, IEEE, 2007.

[5] C. Byrnes, F. Priscoli, and A. Isidori, *Output Regulation of Uncertain Nonlinear Systems*. Birkhauser Basel, 1997.

[6] A. D. Kuo, "Choosing your steps carefully," *IEEE Robotics & Automation Magazine*, vol. 14, no. 2, pp. 18–29, 2007.

[7] E. Westervelt, J. Grizzle, and D. Koditschek, "Hybrid zero dynamics of planar biped walkers," *IEEE Trans. Auto. Contr.*, vol. 48, no. 1, pp. 42–56, 2003.

[8] A. Mohammadi, M. Maggiore, and L. Consolini, "Dynamic virtual holonomic constraints for stabilization of closed orbits in underactuated mechanical systems," *Automatica*, vol. 94, pp. 112–124, 2018.

[9] G. Pratt, M. M. Williamson, *et al.*, "Series elastic actuators," in *Intelligent Robots and Systems 95.'Human Robot Interaction and Cooperative Robots', Proceedings. 1995 IEEE/RSJ International Conference on*, vol. 1, pp. 399–406, IEEE, 1995.

[10] R. Van Ham, B. Vanderborght, M. Van Damme, B. Verrelst, and D. Lefeber, "Maccepa, the mechanically adjustable compliance and controllable equilibrium position actuator: Design and implementation in a biped robot," *Robotics and Autonomous Systems*, vol. 55, no. 10, pp. 761–768, 2007.

[11] K. Hosoda, T. Takuma, A. Nakamoto, and S. Hayashi, "Biped robot design powered by antagonistic pneumatic actuators for multi-modal locomotion," *Robotics and Autonomous Systems*, vol. 56, no. 1, pp. 46–53, 2008.

[12] A. Spröwitz, A. Tuleu, M. Vespignani, M. Ajallooeian, E. Badri, and A. J. Ijspeert, "Towards dynamic trot gait locomotion: Design, control, and experiments with cheetah-cub, a compliant quadruped robot," *The International Journal of Robotics Research*, vol. 32, no. 8, pp. 932–950, 2013.

[13] J. Buchli, M. Kalakrishnan, M. Mistry, P. Pastor, and S. Schaal, "Compliant quadruped locomotion over rough terrain," in *Intelligent Robots and Systems, 2009. IROS 2009. IEEE/RSJ International Conference on*, pp. 814–820, IEEE, 2009.

[14] R. Skelton and M. de Oliveira, *Tensegrity Systems*. Springer, 2009.

[15] T. Bliss, J. Werly, T. Iwasaki, and H. Bart-Smith, "Experimental validation of robust resonance entrainment for CPG-controlled tensegrity structures," *IEEE Trans. Contr. Sys. Tech.*, vol. 21, no. 3, pp. 666–678, 2012.

[16] T. Bliss, T. Iwasaki, and H. Bart-Smith, "Central pattern generator control of a tensegrity swimmer," *IEEE/ASME Trans. Mechatronics*, vol. 18, no. 2, pp. 586–597, 2013.

[17] P. Beyl, K. Knaepen, S. Duerinck, M. Van Damme, B. Vanderborght, R. Meeusen, and D. Lefeber, "Safe and compliant guidance by a powered knee exoskeleton for robot-assisted rehabilitation of gait," *Advanced Robotics*, vol. 25, no. 5, pp. 513–535, 2011.

[18] H. Vallery, J. Veneman, E. Van Asseldonk, R. Ekkelenkamp, M. Buss, and H. Van Der Kooij, "Compliant actuation of rehabilitation robots," *IEEE Robotics & Automation Magazine*, vol. 15, no. 3, 2008.

[19] S. Kohannim and T. Iwasaki, "Analytical insights into optimality and resonance in fish swimming," *J. Royal Society Interface*, vol. 11, p. 20131073, 2014.

[20] B. Ahlborn and R. Blake, "Walking and running at resonance," *Zoology*, vol. 105, pp. 165–174, 2002.

[21] B. Ahlborn, R. Blake, and W. Megill, "Frequency tuning in animal locomotion," *Zoology*, vol. 109, pp. 43–53, 2006.

[22] E. P. Zehr and J. Duysens, "Regulation of arm and leg movement during human locomotion," *The Neuroscientist*, vol. 10, no. 4, pp. 347–361, 2004.

[23] N. Hatsopoulos and W. W. Jr., "Resonance tuning in rhythmic arm movements," *J. Motor Behavior*, vol. 28, no. 1, pp. 3–14, 1996.
[24] M. Williamson, "Neural control of rhythmic arm movements," *Neural Networks*, vol. 11, pp. 1379–1394, 1998.
[25] T. Iwasaki and M. Zheng, "Sensory feedback mechanism underlying entrainment of central pattern generator to mechanical resonance," *Biological Cybernetics*, vol. 94, no. 4, pp. 245–261, 2006.
[26] B. Verdaasdonk, H. Koopman, and F. V. der Helm, "Resonance tuning in a neuro-musculo-skeletal model of the forearm," *Biological Cybernetics*, vol. 96, no. 2, pp. 165–180, 2007.
[27] C. Williams and S. DeWeerth, "A comparison of resonance tuning with positive versus negative sensory feedback," *Biol. Cyb.*, vol. 96, pp. 603–614, 2007.
[28] Y. Futakata and T. Iwasaki, "Formal analysis of resonance entrainment by central pattern generator," *Journal of mathematical biology*, vol. 57, no. 2, pp. 183–207, 2008.
[29] Y. Futakata and T. Iwasaki, "Entrainment to natural oscillations via uncoupled central pattern generators," *IEEE Trans. Auto. Contr.*, vol. 56, no. 5, pp. 1075–1089, 2011.
[30] J. Zhao and T. Iwasaki, "CPG control for assisting human with periodic motion tasks," in *Decision and Control (CDC), 2016 IEEE 55th Conference on*, pp. 5035–5040, IEEE, 2016.
[31] J. Nakanishi, J. Morimoto, G. Endo, G. Cheng, S. Schaal, and M. Kawato, "Learning from demonstration and adaptation of biped locomotion," *Robotics and Autonomous Systems*, vol. 47, pp. 79–91, 2004.
[32] L. Righetti, J. Buchli, and A. J. Ijspeert, "Dynamic hebbian learning in adaptive frequency oscillators," *Physica D: Nonlinear Phenomena*, vol. 216, no. 2, pp. 269–281, 2006.
[33] J. Buchli, F. Iida, and A. J. Ijspeert, "Finding resonance: Adaptive frequency oscillators for dynamic legged locomotion," in *Intelligent Robots and Systems, 2006 IEEE/RSJ International Conference on*, pp. 3903–3909, IEEE, 2006.
[34] A. Fradkov, "Exploiting nonlinearity by feedback," *Physica D*, vol. 128, pp. 159–168, 1999.
[35] D. Efimov, A. Fradkov, and T. Iwasaki, "Exciting multi-DOF systems by feedback resonance," *Automatica*, vol. 49, no. 6, pp. 1782–1789, 2013.
[36] J. Zhao and T. Iwasaki, "Adaptive natural entrainment via Andronov-Hopf oscillator," in *American Control Conference*, pp. 1257–1262, 2017.
[37] B. Anderson, R. R. Bitmead, C. R. Johnson Jr, P. V. Kokotovic, R. L. Kosut, I. M. Mareels, L. Praly, and B. D. Riedle, *Stability of adaptive systems: Passivity and averaging analysis*. MIT press, 1986.
[38] H. Amann, *Ordinary Differential Equations: An Introduction to Nonlinear Analysis*. Walter de Gruyter, 1990.
[39] H. Khalil, *Nonlinear Systems*. Prentice Hall, 1996.
[40] J. Hauser and C. Chung, "Converse Lyapunov functions for exponentially stable periodic orbits," *Sys. Contr. Lett.*, vol. 23, pp. 27–34, 1994.
[41] P. Hartman, *Ordinary Differential Equations*. John Wiley & Sons, Inc., 1964.
[42] R. Brockett, *Finite Dimensional Linear Systems*. John Wiley & Sons, Inc., 1970.
[43] X. Liu and T. Iwasaki, "Design of coupled harmonic oscillators for synchronization and coordination," *IEEE Transactions on Automatic Control*, 2017. (To appear).
[44] M. Spong and M. Vidyasagar, *Robot Dynamics and Control*. John Wiley & Sons, 1989.
[45] C. Sultan and R. Skelton, "Deployment of tensegrity structures," *International Journal of Solids and Structures*, vol. 40, no. 18, pp. 4637–4657, 2003.

Jinxin Zhao received his Ph.D. degree in Aerospace Engineering from University of California, Los Angeles in 2017. He received his M.S. degree in Aerospace Engineering from University of Michigan, Ann Arbor in 2013 and B.S. degree in Mechanical Engineering from Zhejiang University, China in 2011. His current research interests include adaptive nonlinear oscillators, CPG control of human assistive robots and distributed control.

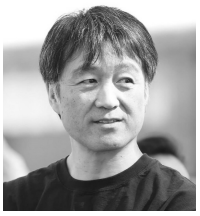

Tetsuya Iwasaki (M'90-SM'01-F'09) received his B.S. and M.S. degrees in Electrical and Electronic Engineering from the Tokyo Institute of Technology (Tokyo Tech) in 1987 and 1990, respectively, and his Ph.D. degree in Aeronautics and Astronautics from Purdue University in 1993. He held a Post-Doctoral Research Associate position at Purdue University (1994-1995), and faculty positions at Tokyo Tech (1995-2000) and at the University of Virginia (2000-2009), before joining the UCLA faculty as Professor of Mechanical and Aerospace Engineering. Dr. Iwasaki's current research interests include dynamics and control of animal locomotion, coupled nonlinear oscillators, global pattern formation via local interactions, and robust/optimal control theories and their applications to engineering systems. He has received CAREER Award from NSF, Pioneer Prize from SICE, George S. Axelby Outstanding Paper Award from IEEE, Rudolf Kalman Best Paper Award from ASME, and Steve Hsia Biomedical Paper Award at the 8th World Congress on Intelligent Control and Automation. He has served as Associate Editor of *IEEE Transactions on Automatic Control*, *Systems & Control Letters*, *IFAC Automatica*, *International Journal of Robust and Nonlinear Control*, and *SIAM Journal on Control and Optimization*.